

Copyright by
Clint R. Hoberg

2011

**The Thesis Committee for Clint Hoberg
Certifies that this is the approved version of the following thesis:**

**Synthesis and Characterization of N-Heterocyclic Phosphenium and
Arsenium Salts**

**APPROVED BY
SUPERVISING COMMITTEE:**

Supervisor:

Alan Cowley

Bradley Holliday

**Synthesis and Characterization of N-Heterocyclic Phosphenium and
Arsenium Salts**

by

Clint R. Hoberg, B. S.

Thesis

Presented to the Faculty of the Graduate School of

The University of Texas at Austin

in Partial Fulfillment

of the Requirements

for the Degree of

Master of Arts

The University of Texas at Austin

May 2011

Abstract

Synthesis and Characterization of N-Heterocyclic Phosphenium and Arsenium Salts

Clint R. Hoberg, M. A.

The University of Texas at Austin, 2011

Supervisor: Alan Cowley

Two ligand types were employed for the one-step preparations of heavy group 15 cations, namely, diazabutadiene (DAB) and bis(imino)acenaphthene (BIAN). By exploiting the redox properties of these ligands, in conjunction with two different synthetic strategies, it was possible to synthesize a variety of phosphenium and arsenium salts in relatively high yields. The first synthetic method took advantage of the known equilibrium between PI/PI_3 in solution. The second synthetic route employed $SnCl_2$ as the reducing agent for converting the reactive trihalides ECl_3 into the corresponding “ECl” moieties ($E = P, As$).

Table of Contents

List of Tables	vii
List of Figures	ix
List of Illustrations	xiii
Synthesis and Characterization of N-Heterocyclic Phosphenium and Arsenium Salts	1
Introduction	1
Results and Discussion	5
Section 1.1: Synthesis of N-Heterocyclic Phosphenium (NHP) Salts ...	5
Synthesis and Characterization of [(<i>t</i> -BuDAB)P] ⁺ [I ₃] ⁻ (4)	8
Synthesis and Characterization of [(<i>p</i> -tolylDAB)P] ⁺ [I ₃] ⁻ (5).....	10
Synthesis and Characterization of [(MesDAB)P] ⁺ [I ₃] ⁻ (6)	10
Synthesis and Characterization of [(DippDAB)P] ⁺ [I ₃] ⁻ (7).....	11
Synthesis and Characterization of [(CyDAB)P] ⁺ [I ₃] ⁻ (8).....	13
Synthesis and Characterization of [(<i>t</i> -BuDAB)P] ⁺ [BPh ₄] ⁻ (11)..	14
Synthesis and Characterization of [(DippDAB)P] ⁺ [BPh ₄] ⁻ (12)..	15
Section 1.2: Synthesis of Phosphenium Cations Containing the BIAN Ligand	17
Synthesis and Characterization of [(DippBIAN)P] ⁺ [SnCl ₅ •THF] ⁻ (13).....	20
Synthesis and Characterization of [(DippBIAN)P] ⁺ [I ₃] ⁻ (14)	22
Synthesis and Characterization of [(DippBIAN)As] ⁺ [SnCl ₅ •THF] ⁻ (15).....	23
Experimental Section	25
General Procedures	25
Physical Measurements.....	25
X-ray Crystallography	26
General Synthetic Procedures for 4-8	26
General Synthetic Procedures for 11 and 12.....	28

Synthesis of [(DippBIAN)P] ⁺ [SnCl ₅ •THF] ⁻	29
Synthesis of [(DippBIAN)P] ⁺ [I ₃] ⁻	30
Synthesis of [(DippBIAN)As] ⁺ [SnCl ₅ •THF] ⁻	30
Tables of Crytsallographic Data	32
References.....	59
Vita	61

List of Tables

Table 1.01. Crystal data and structure refinement for 4.	33
Table 1.02. Selected bond lengths (Å) for 4.	34
Table 1.03. Selected bond angles (°) for 4.	34
Table 1.04. Crystal data and structure refinement for 6.	36
Table 1.05. Selected bond lengths (Å) for 6.	37
Table 1.06. Selected bond angles (°) for 6.	37
Table 1.07. Crystal data and structure refinement for 7.	39
Table 1.08. Selected bond lengths (Å) for 7.	40
Table 1.09. Selected bond angles (°) for 7.	40
Table 1.10. Crystal data and structure refinement for 8.	42
Table 1.11. Selected bond lengths (Å) for 8.	43
Table 1.12. Selected bond angles (°) for 8.	43
Table 1.13. Crystal data and structure refinement for 11.	45
Table 1.14. Selected bond lengths (Å) for 11.	46
Table 1.15. Selected bond angles (°) for 11.	46
Table 1.16. Crystal data and structure refinement for 12.	48
Table 1.17. Selected bond lengths (Å) for 12.	49
Table 1.18. Selected bond angles (°) for 12.	49
Table 1.19. Crystal data and structure refinement for 13.	51
Table 1.20. Selected bond lengths (Å) for 13.	52
Table 1.21. Selected bond angles (°) for 13.	52
Table 1.22. Crystal data and structure refinement for 14.	54
Table 1.23. Selected bond lengths (Å) for 14.	55

Table 1.24. Selected bond angles (°) for 14.	55
Table 1.25. Crystal data and structure refinement for 15.	57
Table 1.26. Selected bond lengths (Å) for 15.	58
Table 1.27. Selected bond angles (°) for 15.	58

List of Figures

Figure 1.01. Example of NHC (1), N-heterocyclic phosphonium cation (2), Triphosphenium cation (3).	1
Figure 1.02. Structures of the DAB and BIAN ligands.	4
Figure 1.03. Molecular structure of 7. The thermal ellipsoids are shown at the 40% probability level. All hydrogen atoms have been omitted for clarity.	6
Figure 1.04. Molecular structure of 8. The thermal ellipsoids are shown at the 40% probability level. All hydrogen atoms have been omitted for clarity.	7
Figure 1.05. Molecular structure of 11. The thermal ellipsoids are shown at the 40% probability level. All hydrogen atoms have been omitted for clarity.	8
Figure 1.06. Molecular structure of 4 showing a partial numbering scheme. The thermal ellipsoids are shown at the 40% probability level. All hydrogen atoms and the I₃⁻ counter-anion have been omitted for clarity.	9
Figure 1.07. Molecular structure of 6 showing a partial numbering scheme. The thermal ellipsoids are shown at the 40% probability level. All hydrogen atoms and the I₃⁻ counter-anion have been omitted for clarity.	11

Figure 1.08. Molecular structure of 7 showing a partial numbering scheme. The thermal ellipsoids are shown at the 40% probability level. All hydrogen atoms and the I₃⁻ counter-anion have been omitted for clarity.	13
Figure 1.09. Molecular structure of 8 showing a partial numbering scheme. The thermal ellipsoids are shown at the 40% probability level. All hydrogen atoms and the I₃⁻ counter-anion have been omitted for clarity.	14
Figure 1.10. Molecular structure of 11 showing a partial numbering scheme. The thermal ellipsoids are shown at the 40% probability level. All hydrogen atoms and the BPh₄⁻ counter-anion have been omitted for clarity.	15
Figure 1.11. Molecular structure of 12 showing a partial numbering scheme. The thermal ellipsoids are shown at the 40% probability level. All hydrogen atoms and the BPh₄⁻ counter-anion have been omitted for clarity.	16
Figure 1.12. Depiction of previously reported phosphonium^{5,14} and arsenium cation¹⁶.	19
Figure 1.13. Molecular structure of 15. The thermal ellipsoids are shown at the 40% probability level. All hydrogen atoms have been omitted for clarity.	19
Figure 1.14. Molecular structure of 13 showing a partial numbering scheme. The thermal ellipsoids are shown at the 40% probability level. All hydrogen atoms have been omitted for clarity.	21

Figure 1.15. Molecular structure of 14 showing a partial numbering scheme. The thermal ellipsoids are shown at the 40% probability level. All hydrogen atoms and the I_3^- counter-anion have been omitted for clarity.	23
Figure 1.16. Molecular structure of 15 showing a partial numbering scheme. The thermal ellipsoids are shown at the 40% probability level. All hydrogen atoms and the $SnCl_5^-$ counter-anion have been omitted for clarity.	24
Figure 1.17. Molecular structure of 4 showing a partial numbering scheme. The thermal ellipsoids are shown at the 40% probability level. All hydrogen atoms and the I_3^- counter-anion have been omitted for clarity.	32
Figure 1.18. Molecular structure of 6 showing a partial numbering scheme. The thermal ellipsoids are shown at the 40% probability level. All hydrogen atoms and the I_3^- counter-anion have been omitted for clarity.	35
Figure 1.19. Molecular structure of 7 showing a partial numbering scheme. The thermal ellipsoids are shown at the 40% probability level. All hydrogen atoms and the I_3^- counter-anion have been omitted for clarity.	38
Figure 1.20. Molecular structure of 8 showing a partial numbering scheme. The thermal ellipsoids are shown at the 40% probability level. All hydrogen atoms and the I_3^- counter-anion have been omitted for clarity.	41

Figure 1.21. Molecular structure of 11 showing a partial numbering scheme. The thermal ellipsoids are shown at the 40% probability level. All hydrogen atoms and the BPh₄⁻ counter-anion have been omitted for clarity.	44
Figure 1.22. Molecular structure of 12 showing a partial numbering scheme. The thermal ellipsoids are shown at the 40% probability level. All hydrogen atoms and the BPh₄⁻ counter-anion have been omitted for clarity.	47
Figure 1.14. Molecular structure of 13 showing a partial numbering scheme. The thermal ellipsoids are shown at the 40% probability level. All hydrogen atoms have been omitted for clarity.	50
Figure 1.15. Molecular structure of 14 showing a partial numbering scheme. The thermal ellipsoids are shown at the 40% probability level. All hydrogen atoms and the I₃⁻ counter-anion have been omitted for clarity.	53
Figure 1.16. Molecular structure of 15 showing a partial numbering scheme. The thermal ellipsoids are shown at the 40% probability level. All hydrogen atoms and the SnCl₅⁻ counter-anion have been omitted for clarity.	56

List of Illustrations

Scheme 1.01. Previously reported synthesis of a phosphenium cation.	2
Scheme 1.02. Schmidpeter <i>et al.</i> route to triphosphenium cations.	3
Scheme 1.03. Synthesis of NHPs via the reaction of PI₃ with the appropriate DAB ligand.	5
Scheme 1.04. Burford <i>et al.</i> reported reaction of a phosphenium cation with a tetraphenylborate anion.	8
Scheme 1.05. Synthesis of an N-heterocyclic group 15 salt via the reaction of ECl₃/SnCl₂ with the appropriate BIAN ligand.	17
Scheme 1.06. Synthesis of an N-heterocyclic group 15 salt via the reaction of EI₃ with the appropriate BIAN ligand.	17

Synthesis and Characterization of N-Heterocyclic Phosphenium and Arsenium Salts

INTRODUCTION

N-Heterocyclic group 15 cations have attracted recent attention because of their isovalent relationship to N-heterocyclic carbenes (NHCs) **1** and their heavier group 14 analogues.¹⁻³ Due to their strong σ -donor and weak π -acceptor properties, NHCs continue to play a prominent role in terms of supporting catalytically relevant transition-metal complexes.⁴ In contrast, the N-heterocyclic group 15 analogues, commonly known as phosphenium cations **2** possess poor σ -donor and strong π -acceptor properties.⁵ As a consequence, transition-metal complexes supported by ligands of this type may exhibit enhanced electrophilicity.⁶⁻⁹

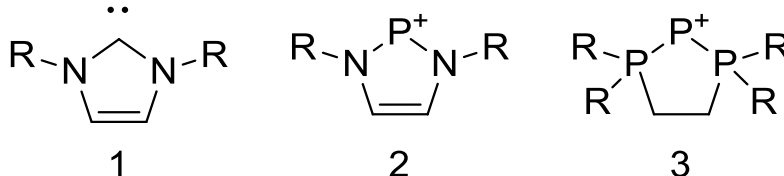
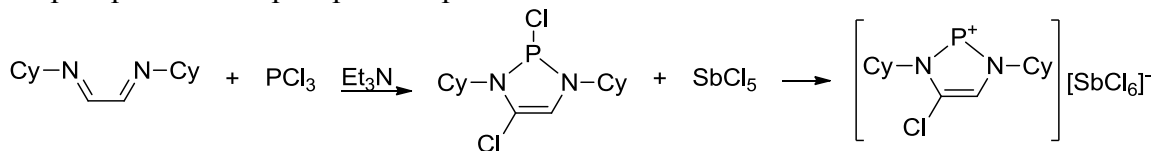


Figure 1.01. Example of NHC (1), N-heterocyclic phosphenium cation (2), Triphosphenium cation (3).

Although the chemistry of NHCs has been explored extensively over the past decade, it is interesting to note that a structurally authenticated N-heterocyclic phosphenium (NHP) was reported¹⁰ prior to the first NHC.¹¹ This phosphenium salt was successfully synthesized in 73% yield via the reaction of $\text{CyN}=\text{CHCH}=\text{NCy}$ with PCl_3 in the presence of Et_3N , followed by treatment with SbCl_5 , thus forming the hexachloroantimonate salt (Scheme 1.01).¹² It was also noted that halide ion abstractions could also be performed by using other Lewis acids such as GaCl_3 .^{13,14} The yields for the halide abstraction step in this reaction pathway are typically >90%. Unfortunately, as

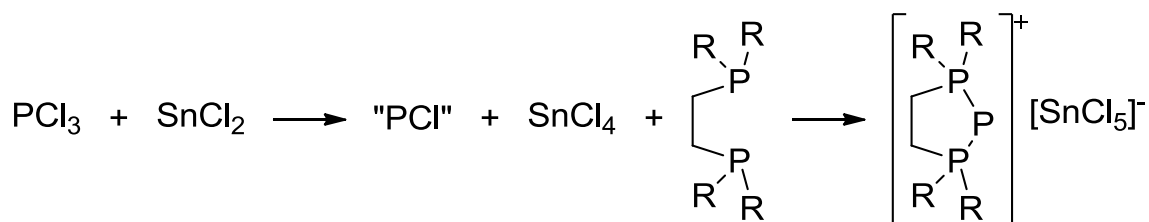
reported in previous work,^{10,12} the yields are significantly more modest overall due to the fact that one or two lower yielding steps are required for conversion of the diimine into the phosphorus-halo phospholene precursor.



Scheme 1.01. Previously reported synthesis of a phosphonium cation.

Similarly, the conversion of phosphorus-halo phospholenes into the corresponding N-heterocyclic phosphonium salts via the metathetical reaction with, e.g., AgPF_6 ,^{13,14} or by means of a Me_3SiCl elimination reaction with Me_3SiOTf also result in modest overall yields.¹⁵ An alternative method of generating the phosphorus-chloro compound was accomplished via the salt elimination reaction of $\text{LiN}(t\text{-Bu})\text{C}=\text{CN}(t\text{-Bu})\text{Li}$ with PCl_3 . However, once again, the overall yield was relatively poor (55%).¹⁶ On the other hand, if dilithium salts are first quenched by protonation with Et_3NHCl and the resulting R-aminoaldimines are subsequently treated with PCl_3 in the presence of Et_3N , the overall yields can be increased to 70-80%.¹⁷ Conversion to the corresponding triflate salts can be achieved in >85% yields.⁵

Pioneering work by Schmidpeter *et al.*,¹⁸ established that the reduction of PCl_3 with SnCl_2 in the presence of chelating bis(phosphines) results in so-called triphosphenium salts in which the central phosphorus atom possesses a formal +1 oxidation state.



Scheme 1.02. Schmidpeter *et al.* route to triphosphenium cations.

While the mechanism of formation of these triphosphenium ions has not been established, it is reasonable to assume that the redox reaction $\text{PCl}_3 + \text{SnCl}_2 \rightarrow \text{"PCI"} + \text{SnCl}_4$ is followed by chloride ion transfer to SnCl_4 from either free or chelated "PCI" (Scheme 1.02). Schmidpeter *et al.*,¹⁹ also demonstrated that acyclic analogues of **3** can be isolated when two monodentate tertiary phosphines are used in place of a chelating bis(phosphine). Interest in the general area of P^+ chemistry has been rekindled recently, not only in terms of the variety of chelating phosphines that are capable of trapping this univalent cation,^{20,21} but also from the standpoint of new methods of generation. For example, Macdonald *et al.*²² have shown that NHCs are capable of both reducing PCl_3 and trapping the resulting P^+ entity as cations of the type $[(\text{NHC})\rightarrow\text{P}\leftarrow(\text{NHC})]^+$. Moreover, this same group^{23,24} established that chelating bis(phosphines) will cause disproportionation of PI_3 , thus forming the iodide salt of **3** along with molecular iodine. Typically, the $^{31}\text{P}\{^1\text{H}\}$ chemical shifts of the central phosphorus atoms of cyclic triphosphenium cations fall in the range of δ : -210 to -270. Moreover, in the case of **3** ($\text{R} = \text{Ph}$), the central phosphorus atom is sufficiently basic to undergo protonation,²⁵ hence these salts are best regarded as adducts of phosphorus(I), namely, the predominant canonical form is $\text{D}^+ \rightarrow \text{P}^- \leftarrow \text{D}^+$ ($\text{D} = \text{phosphine, NHC}$).

Given the foregoing, the work presented in the present chapter is concerned with an exploration of the consequences of trapping the putative EX ($\text{E} = \text{P, As}$; $\text{X} = \text{halogen}$)

molecules with ligands other than phosphines and carbenes. The first such ligand class is based on the diazabutadiene (DAB) framework. The DAB ligand has been used extensively for the support of a variety of transition metal complexes. However, one of the inherent drawbacks of using the DAB ligand is the degradation of DAB-supported catalysts by cleavage of the diimine C-C bond. As a consequence, it was necessary to develop a new class of supporting ligand. The so-called 1,2-bis(arylimino)acenaphthene (aryl-BIAN) ligand features an extensive π -system and two Lewis basic sites. Interestingly, the aryl-BIAN class of ligands is able to function as both electron and proton sponges. For example, it has been found the aryl-BIAN ligand will sequentially add four electrons. In one remarkable case, each of the four reduced species was structurally authenticated.²⁶ The extended π -system of the BIAN ligand also has the added benefit of withdrawing more electron density away from the metal center in complexes that are supported by this ligand. This desirable combination of properties has resulted in the widespread use of aryl-BIAN-supported transition metal derivatives as versatile catalysts for a variety of important reactions, particularly olefin polymerization.²⁷⁻²⁹ In stark contrast, considerably less information is available regarding aryl-BIAN complexes of the main group elements.³⁰ When the previous work was started, this ligand class had not been used in the context of group 15 chemistry.

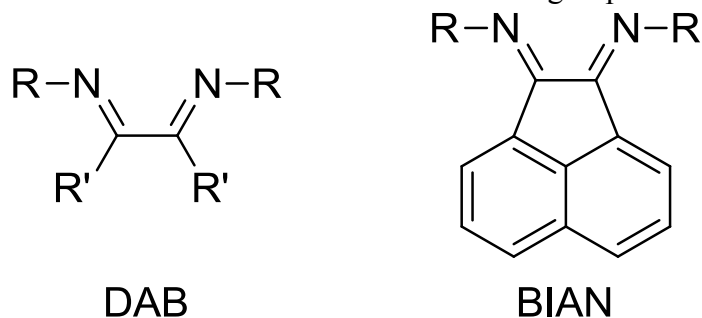
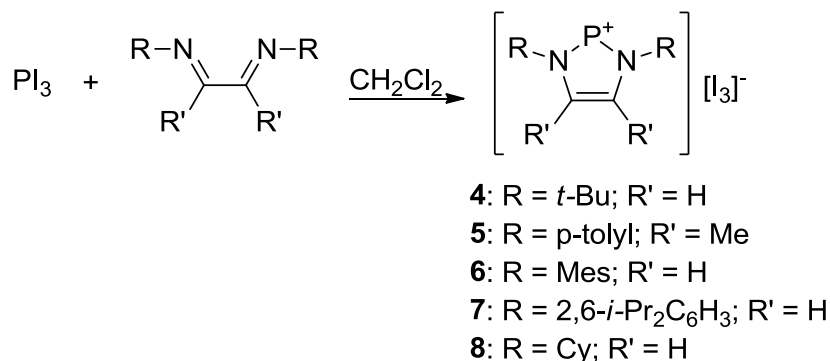


Figure 1.02. Structures of the DAB and BIAN ligands.

RESULTS AND DISCUSSION

Section 1.1: Synthesis of N-Heterocyclic Phosphenium (NHP) Salts



Scheme 1.03. Synthesis of NHPs via the reaction of PI₃ with the appropriate DAB ligand.

As summarized in Scheme 1.03, the triiodide salts of *N*-alkyl and *N*-aryl-substituted N-heterocyclic phosphonium cations can be readily prepared in one step via the reaction of PI₃ with the appropriate diimine in CH₂Cl₂ solution. In each case, the yield of crude product is >80% and recrystallization results in 80-90% yields of red crystals of triiodide salts **4-8**. The phosphonium cations in **5-8** have not been reported previously. However, the 4-chloro analogues of **6**⁵ and **8**¹⁰ have been prepared and structurally characterized, as has the 3,4-dimethyl analogue of **6**.³¹ Compounds **4-8** were characterized by ¹H, ¹³C{¹H}, and ³¹P{¹H} NMR spectroscopy in conjunction with high-resolution mass spectrometry (HRMS). The ³¹P{¹H} NMR chemical shifts for **4-8**, which fall in the range δ: 200-230 ppm, are diagnostic of the presence of phosphonium cations¹⁻³ and thus supportive of the structural formula depicted in Scheme 1.03. Moreover, the CI mass spectra of **4-8** evidence a 100% abundance peak corresponding to the phosphonium

ion in each case. Structural confirmation was provided by single-crystal X-ray diffraction studies of **4** and **6-8**. The metrical parameters for the phosphonium cations are very similar. The structures of **7** and **8**, which are representative of the other cations, are displayed in Figures 1.03 and 1.04, respectively. Akin to other phosphonium cation structures, the ring C-C bond distances, which range in length from 1.342(6) to 1.353(6) Å, are shorter than those of typical C-C single bond distances and the C-N bond distances, which range from 1.366(5) to 1.400(5) Å, correspond to a bond order of approximately 1. It is clear from the foregoing spectroscopic and structural data that the phosphorus atom adopts the +3 oxidation state in **4-8**. At this point, there is no mechanistic information regarding the diimine/PI₃ reactions. However, one scenario is that the interaction of the diimine with PI₃ results initially in the formation of I₂ and a donor-acceptor complex between the R-diimine and PI, from which I⁻ is abstracted by I₂. The process is then completed by the subsequent or concomitant transfer of two electrons from the P⁺ moiety into the LUMO of the R-diimine.

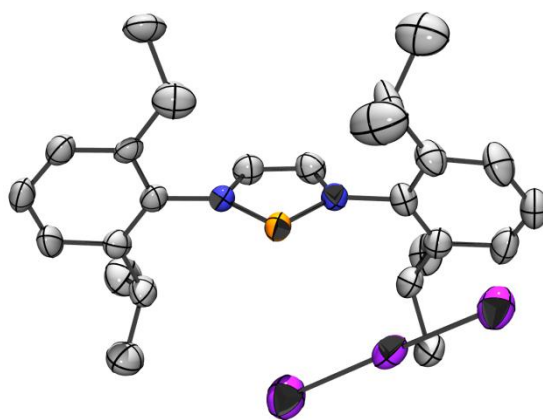


Figure 1.03. Molecular structure of 7. The thermal ellipsoids are shown at the 40% probability level. All hydrogen atoms have been omitted for clarity.

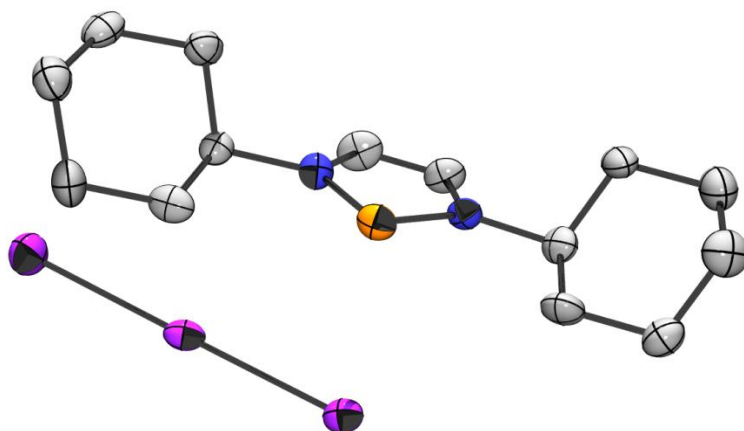


Figure 1.04. Molecular structure of **8. The thermal ellipsoids are shown at the 40% probability level. All hydrogen atoms have been omitted for clarity.**

Further synthetic utility is conferred on this synthetic method by the observation that **4-8** undergo facile anion exchange reactions with, *e.g.*, $\text{NaB}(\text{C}_6\text{H}_5)_4$ to afford the corresponding tetraphenylborate salts in virtually quantitative yields. Two such salts have been structurally authenticated, namely, **11** and **12**. The structure of **11** is illustrated in Figure 1.05. The structures of tetraphenylborate salts of phosphonium ions are of particular interest because of the report by Burford *et al.*³² that **9** undergoes phenyl back-transfer and $\text{B}(\text{C}_6\text{H}_5)_3$ coordination to form the covalent phosphine-borane complex **10** (Scheme 1.04). Because the acyclic phosphonium salt $[(i\text{-Pr}_2\text{N})_2\text{P}][\text{B}(\text{C}_6\text{H}_5)_4]$ does not undergo such a transformation, these authors suggested that, in this case, the *N-isopropyl* groups provided a sufficient steric barrier to preclude this type of reaction. The structures of **11** and **12**, which feature bulky *t*-Bu and 2,6-*i*-Pr₂C₆H₃ groups, respectively, exhibit no close anion-cation contacts, thus supporting the view of Burford *et al.*³² As expected, the metrical parameters for the phosphonium cations in **11** and **12** are identical within experimental error with those in the triiodide salts **4** and **7**, respectively.

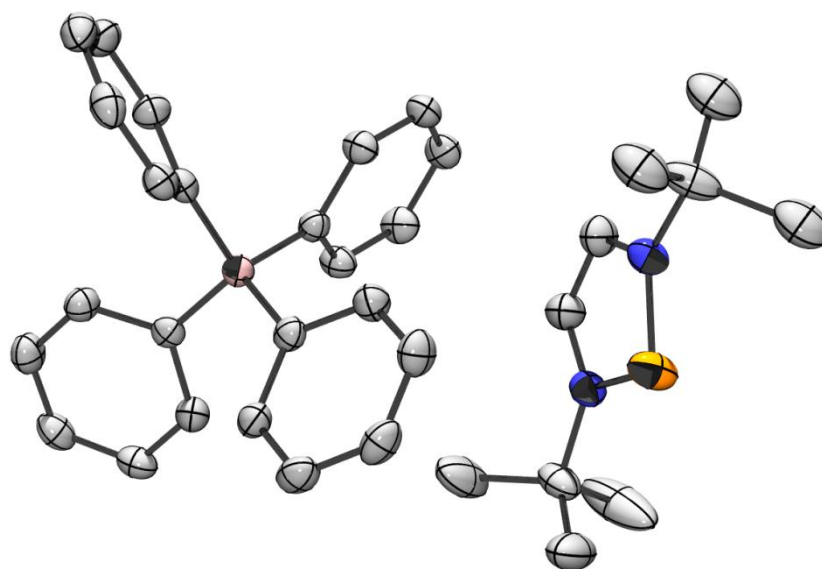
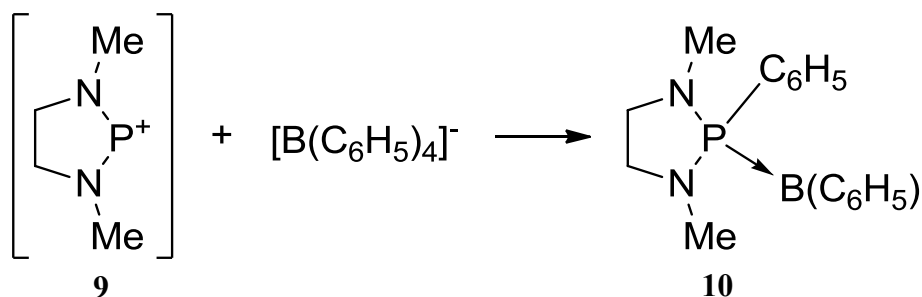


Figure 1.05. Molecular structure of 11. The thermal ellipsoids are shown at the 40% probability level. All hydrogen atoms have been omitted for clarity.



Scheme 1.04. Burford *et al.* reported reaction of a phosphonium cation with a tetraphenylborate anion.

Synthesis and Characterization of [(t-BuDAB)P]⁺[I₃]⁻ (4)

The phosphonium salt [(t-BuDAB)P]⁺[I₃]⁻ (4) was synthesized by dropwise addition of a solution of PI₃ in 30 mL of CH₂Cl₂ to a solution of t-BuDAB in 30 mL of CH₂Cl₂ over a period of 30 min. The resulting red-brown reaction mixture was stirred for an additional 12 h and subsequently filtered through Celite®. Workup of the reaction mixture and removal of the solvent under reduced pressure resulted in the isolation of an analytically pure dark brown powder (yield = 84%). Recrystallization of the crude

product from a dichloromethane/hexane (2:1) mixture at $-40\text{ }^{\circ}\text{C}$ under an argon atmosphere yielded dark brown crystals suitable for X-ray diffraction experiments. A single-crystal X-ray diffraction study confirmed the identity of the title compound and is displayed in Figure 1.06. Details of the data collection, structure solution and refinement are presented in Table 1.01 and a selection of metrical parameters is listed in Tables 1.02 and 1.03.

Compound **4** crystallizes in the space group $P2_1/c$. Metrical parameters which are pertinent to the description of the structure of **4** include the C(1)-C(2) bond distance of $1.353(6)\text{ \AA}$, which is indicative of a C-C double bond, and the average C-N bond distance of $1.366(5)\text{ \AA}$ which implies a bond order of one. As expected, these metrical parameters are similar to those of previously reported N-heterocyclic phosphonium salts.

The ^{31}P NMR spectrum of **4** revealed the presence of a signal at δ : 204.3. The chemical shift of this signal is indicative of the presence of a phosphonium cation and is consistent with those of previously reported examples.

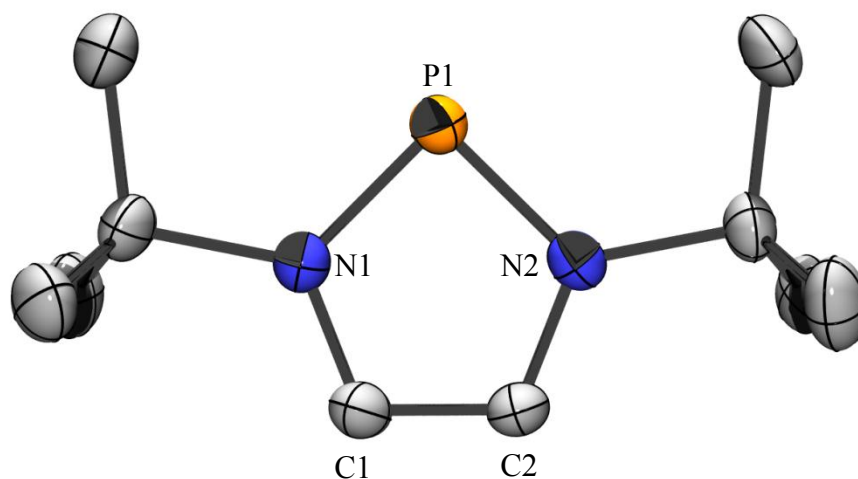


Figure 1.06. Molecular structure of **4** showing a partial numbering scheme. The thermal ellipsoids are shown at the 40% probability level. All hydrogen atoms and the I_3^- counter-anion have been omitted for clarity.

Synthesis and Characterization of [(p-tolylDAB)P]⁺[I₃]⁻ (5)

The phosphonium salt [(p-tolylDAB)P]⁺[I₃]⁻ (**5**) was prepared by dropwise addition of a solution of PI₃ in 30 mL of CH₂Cl₂ to a solution of p-tolylDAB in 30 mL of CH₂Cl₂ over a period of 30 min. The resulting red-brown reaction mixture was stirred for 12 h, following which it was then filtered through Celite®. Workup of the reaction mixture and removal of solvent resulted in the isolation of an analytically pure dark brown powder (yield = 88%). Despite several attempted recrystallizations, it was not possible to isolate crystalline material suitable for X-ray crystallography. As a consequence the identification of this compound is based on NMR and mass spectroscopic data.

The ³¹P{¹H} NMR spectrum revealed the presence of a signal at δ: 227.1, which falls within the ³¹P chemical shift range anticipated for a phosphonium cation and is consistent with those of previously reported examples. The high resolution mass spectrum was recorded for this compound using a chemical ionization technique with methane gas plasma as the ionization source. The parent peak with 100% abundance corresponds to a *m/z* of 295.1364 which is consistent with the calculated value of *m/z*: 295.1364.

Synthesis and Characterization of [(MesDAB)P]⁺[I₃]⁻ (6)

The phosphonium salt [(MesDAB)P]⁺[I₃]⁻ (**6**) was synthesized by dropwise addition of a solution of PI₃ in 30 mL of CH₂Cl₂ to a solution of MesDAB in 30 mL of CH₂Cl₂ over a period of 30 min. The resulting red-brown reaction mixture was stirred for 12 h, following which it was filtered through Celite®. Workup of the reaction mixture and removal of solvent resulted in the isolation of an analytically pure brown powder (yield = 87%). Recrystallization from a 2:1 dichloromethane/hexane mixture at -40 °C under an argon atmosphere resulted in a crop of brown crystals suitable for X-ray

diffraction experiments. A single crystal X-ray diffraction study confirmed the identity of the title compound to be that shown in Figure 1.07. Details of the data collection, structure solution and refinement are compiled in Table 1.04 and a selection of metrical parameters listed in Tables 1.05 and 1.06.

Compound **6** crystallizes in the monoclinic space group $C2/c$. Metrical parameters which are pertinent to the description of the structure of **6** include the C(1)-C(2) bond distance of 1.342(9) Å, which is indicative of a C-C double bond, and the average C-N bond distance of 1.371(6) Å which implies a bond order of one. As expected, these metrical parameters are similar to those of previously reported N-heterocyclic phosphonium cations.

The $^{31}\text{P}\{^1\text{H}\}$ NMR spectrum revealed the presence of a signal located at δ : 209.7. The chemical shift of this signal is indicative of the presence of a phosphonium cation and is consistent with those of previously reported examples.

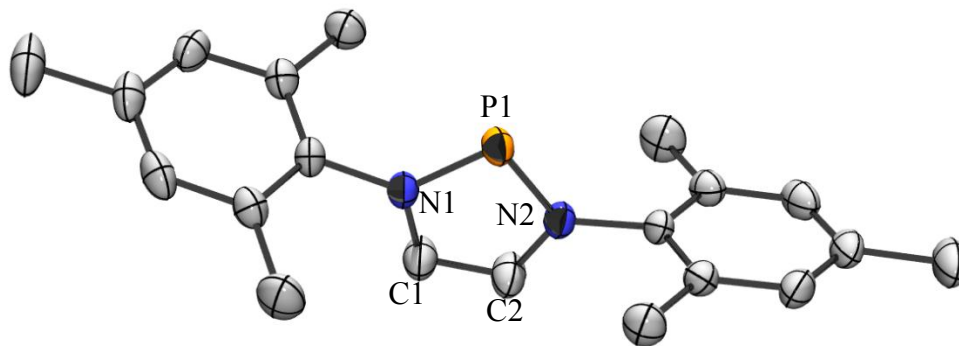


Figure 1.07. Molecular structure of **6 showing a partial numbering scheme. The thermal ellipsoids are shown at the 40% probability level. All hydrogen atoms and the I_3^- counter-anion have been omitted for clarity.**

Synthesis and Characterization of [(DippDAB)P]⁺[I₃]⁻ (7)

The phosphonium salt [(DippDAB)P]⁺[I₃]⁻ (**7**) was prepared by dropwise addition of a solution of PI₃ in 30 mL of CH₂Cl₂ to a solution of DippDAB in 30 mL of CH₂Cl₂

over a period of 30 min. The resulting red/brown reaction mixture was stirred for 12 h, then filtered through Celite. Workup of the reaction mixture and removal of solvent at reduced pressure resulted in the isolation of **7** as an analytically pure brown powder (92%). Recrystallization of **7** from a 2:1 dichloromethane/hexane solvent mixture at -40 °C under an argon atmosphere yielded a crop of brown crystals suitable for X-ray diffraction experiments. The identity of the title compound as shown in Figure 1.08 was established on the basis of a single-crystal X-ray diffraction study. Details of the data collection, structure solution and refinement are compiled in Table 1.07 and a selection of metrical parameters is presented in Tables 1.08 and 1.09.

Compound **7** crystallizes in the triclinic space group *P1*. The metrical parameters which are pertinent to the description of the structure of **7** include the C(1)-C(2) bond distance of 1.342(9) Å, which is indicative of a C-C double bond, and the average C-N bond distance of 1.388(6) Å which implies a bond order of one. As expected, these metrical parameters are similar to those of previously reported N-heterocyclic phosphonium cations.

The $^{31}\text{P}\{^1\text{H}\}$ NMR spectrum revealed the presence of a signal located at δ : 207.4. The chemical shift of this signal is indicative of the presence of a phosphonium cation and is consistent with those of previously reported examples.

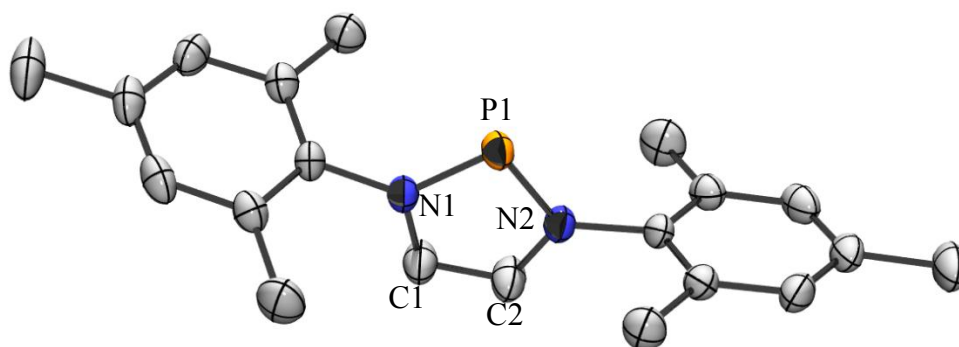


Figure 1.08. Molecular structure of **7** showing a partial numbering scheme. The thermal ellipsoids are shown at the 40% probability level. All hydrogen atoms and the I_3^- counter-anion have been omitted for clarity.

*Synthesis and Characterization of [(CyDAB)P]⁺[I₃]⁻ (**8**)*

The phosphonium salt [(CyDAB)P]⁺[I₃]⁻ (**8**) was synthesized by dropwise addition of a solution of PI₃ in 30 mL of CH₂Cl₂ to a solution of CyDAB in 30 mL of CH₂Cl₂ over a period of 30 min. The resulting red-brown reaction mixture was stirred for 12 h prior to filtration through Celite®. Workup of the reaction mixture and removal of solvent resulted in the isolation of **8** as an analytically pure dark brown powder (yield = 81%). Recrystallization from a 2:1 dichloromethane/hexane mixture at -40 °C under an argon atmosphere afforded a crop of brown crystals suitable for X-ray diffraction experiments. A single crystal X-ray diffraction study confirmed the identity of the title compound to be that shown in Figure 1.09. Details of the data collection, structure solution and refinement are compiled in Table 1.10 and a selection of metrical parameters appears in Tables 1.11 and 1.12.

Compound **8** crystallizes in the monoclinic space group *P1*. The metrical parameters which are pertinent to the description of the structure of **8** include the C(1)-C(2) bond distance of 1.344(17) Å, which is indicative of a C-C double bond, and the average C-N bond distance of 1.379(15) Å which implies a bond order of one. As

expected, these metrical parameters are similar to those of previously reported N-heterocyclic phosphonium cations.

The $^{31}\text{P}\{^1\text{H}\}$ NMR spectrum revealed the presence of a signal located at δ : 209.9. The chemical shift of this signal is indicative of the presence of a phosphonium cation and is consistent with those of previously reported examples.

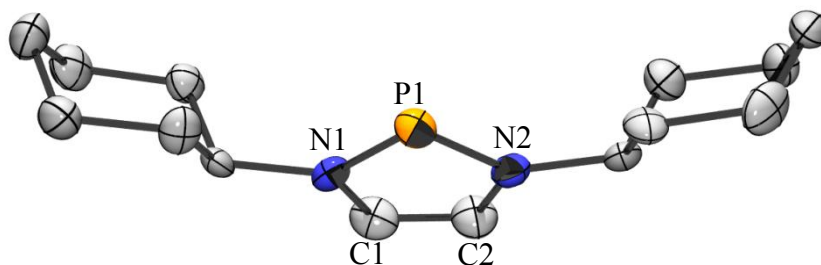


Figure 1.09. Molecular structure of **8** showing a partial numbering scheme. The thermal ellipsoids are shown at the 40% probability level. All hydrogen atoms and the I_3^- counter-anion have been omitted for clarity.

*Synthesis and Characterization of [(*t*-BuDAB)P] $^+$ [BPh $_4$] $^-$ (**11**)*

A mixture of **4** and NaBPh $_4$ in 50 mL of THF solution was stirred at room temperature for 12 h. All the volatiles were removed under reduced pressure, and the resulting yellow residue was extracted with 30 mL of CH $_2$ Cl $_2$ to give a clear light-yellow solution. Slow evaporation of the solvent under an argon atmosphere resulted in the isolation of the crystalline tetraphenylborate salt **11** in virtually quantitative yield. Details of the data collection, structure solution and refinement are compiled in Table 1.13 and a selection of metrical parameters is presented in Tables 1.14 and 1.15.

Compound **11** crystallizes in the orthorhombic space group *Pbca*. The metrical parameters which are pertinent to the description of the structure of **11** include the C(1)-C(2) bond distance of 1.352(4) Å, which is indicative of a C-C double bond, and the average C-N bond distance of 1.368(3) Å which implies a bond order of one. As

expected, these metrical parameters are similar to those of previously reported N-heterocyclic phosphonium cations.

$^{31}\text{P}\{^1\text{H}\}$ NMR analysis revealed the presence of a signal located at δ : 202.5. The chemical shift of this signal is indicative of the presence of a phosphonium cation and is consistent with those of previously reported examples.

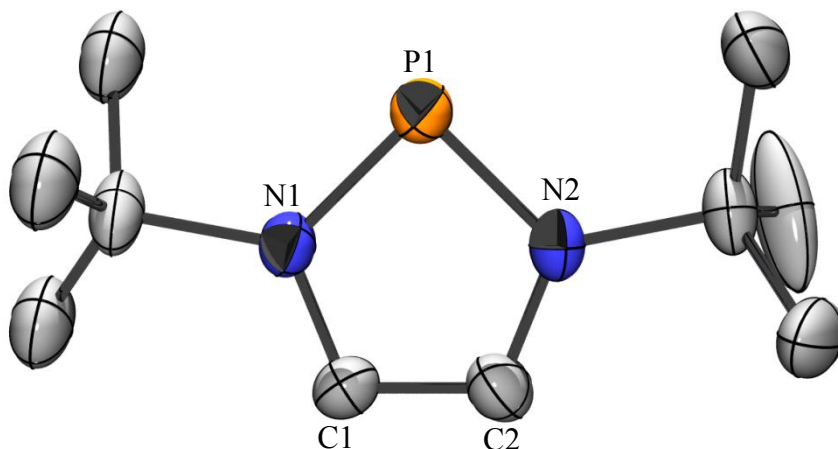


Figure 1.10. Molecular structure of 11 showing a partial numbering scheme. The thermal ellipsoids are shown at the 40% probability level. All hydrogen atoms and the BPh_4^- counter-anion have been omitted for clarity.

Synthesis and Characterization of $[(\text{DippDAB})\text{P}]^+[\text{BPh}_4]^-$ (12)

A mixture of **7** and NaBPh_4 in 50 mL of THF solution was stirred at room temperature for 12 h. All the volatiles were removed under reduced pressure, and the resulting yellow residue was extracted with 30 mL of CH_2Cl_2 to give a clear light-yellow solution. Slow evaporation of the solvent under an argon atmosphere resulted in the isolation of the crystalline tetraphenylborate salt **12** in virtually quantitative yield. Details of the data collection, structure solution and refinement are compiled in Table 1.16 and a selection of metrical parameters is presented in Tables 1.17 and 1.18.

Compound **12** crystallizes in the monoclinic space group $P2_1/c$. Metrical parameters which are pertinent to the description of the structure of **12** include the C(1)-

C(2) bond distance of 1.355(3) Å, which is indicative of a C-C double bond, and the average C-N bond distance of 1.379(3) Å which implies a bond order of one. As expected, these metrical parameters are similar to those of previously reported N-heterocyclic phosphonium cations.

$^{31}\text{P}\{^1\text{H}\}$ NMR analysis revealed the presence of a signal located at δ : 202.5. The chemical shift of this signal is indicative of the presence of a phosphonium cation and is consistent with those of previously reported examples.

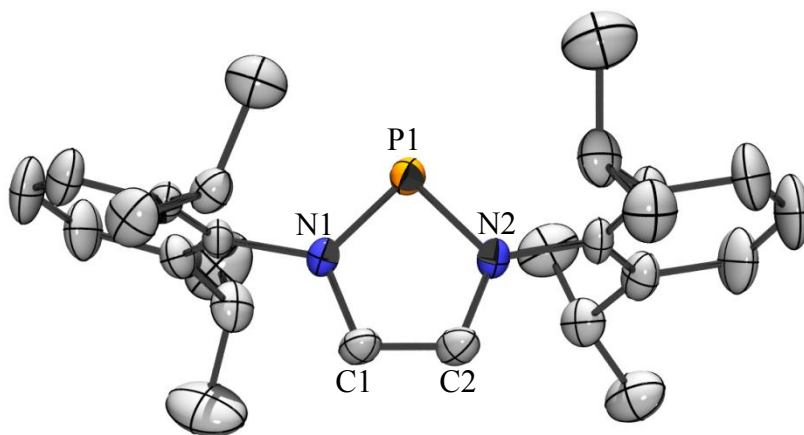
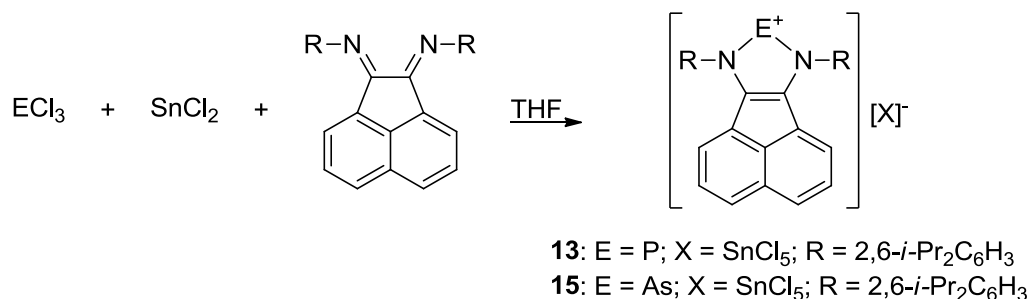
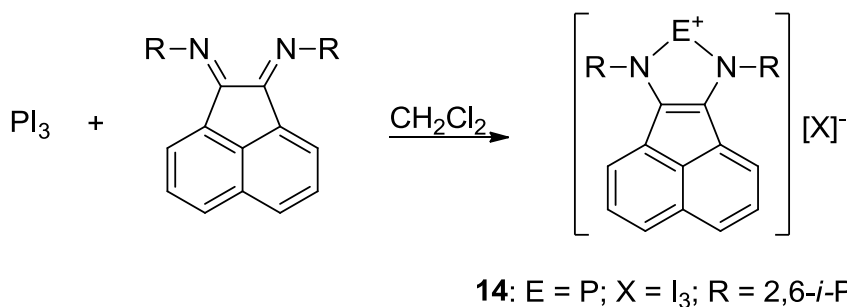


Figure 1.11. Molecular structure of 12 showing a partial numbering scheme. The thermal ellipsoids are shown at the 40% probability level. All hydrogen atoms and the BPh_4^- counter-anion have been omitted for clarity.

Section 1.2: Synthesis of Phosphenium Cations Containing the BIAN Ligand



Scheme 1.05. Synthesis of an N-heterocyclic group 15 salt via the reaction of ECl₃/SnCl₂ with the appropriate BIAN ligand.



Scheme 1.06. Synthesis of an N-heterocyclic group 15 salt via the reaction of EI₃ with the appropriate BIAN ligand.

As summarized in Scheme 1.05, the pentachlorostannate salts of *N*-aryl-substituted N-heterocyclic phosphenium and arsenium cations can be readily prepared by the one pot reaction of ECl₃/SnCl₅ (E = P, As) with the appropriate BIAN ligand in THF solution. In each case, the yield of crude product fell in the range 66-90%. Recrystallization resulted in the isolation of 50-80% yields of green crystals in the case of pentachlorostannate salts **13** and **15**, along with a crop of red-brown crystals of **14**. The phosphenium and arsenium cations in **13-15** have not been reported previously. Compounds **13** and **14** were characterized on the basis of ¹H, ¹³C{¹H}, and ³¹P{¹H} NMR spectroscopy in conjunction with high-resolution mass spectrometry (HRMS). The ³¹P NMR chemical shifts for **13** and **14**, which fall in the range δ: 230-240 ppm, are

diagnostic of the presence of phosphonium cations and thus supportive of the structural formula depicted in Scheme 1.05.^{1,2} Moreover, the CI mass spectra of **13-15** evidence a 100% abundance peak corresponding to the parent ion in each case. The most noteworthy structural features concern the C-C and C-N bond distances within the planar PN₂C₂ ring. Specifically, the C(1)-C(12) bond distance (1.395(5) Å) is considerably shorter than the corresponding distance in the uncoordinated dpp-BIAN ligand (1.527 Å) and indicative of double bond character.^{33,34} Moreover, the C-N bond distances in **13** (av. 1.385(5) Å) are longer than those in free dpp-BIAN (1.272 Å) and commensurate with a bond order of approximately one.^{33,34} Furthermore, the structure of the dpp-BIAN ligand in **13** also bears a close resemblance to that of the complex [(dtb-BIAN)Mg(THF)₂] which was isolated from the reaction of activated Mg metal with the neutral dtb-BIAN ligand (2,5-di-*tert*-butylphenyl).³⁵ Thus, akin to Mg metal, the “PCI” molecule functions as a two-electron reductant toward the aryl-BIAN ligand. Accordingly, and in contrast to **3** and related triphosphenium cations, the dicoordinate phosphorus atom of **13** adopts the +3 rather than the +1 oxidation state. The fact that internal redox takes place in the case of **13** but not **3** is attributable to the presence of a low-lying LUMO in the neutral dpp-BIAN ligand and the aromaticity of the resulting [(dpp-BIAN)]²⁻ anion. The [SnCl₅THF]⁻ counter anion adopts an essentially octahedral geometry and the closest P-Cl contacts are to Cl(1) (3.374(5) Å) and Cl(2) (3.328(5) Å).

The ambient temperature reaction of equimolar quantities of dpp-BIAN and PI₃ in CH₂Cl₂ solution in the absence of a reducing agent was also investigated. ³¹P{¹H} NMR spectroscopic assay of the resulting dark brown reaction mixture revealed the exclusive presence of a sharp singlet at δ: 234.5. That virtually quantitative formation of [(dpp-BIAN)P][I₃] **14** had occurred was confirmed on the basis of ¹H and ¹³C{¹H} NMR spectroscopic data along with an X-ray diffraction study of a single crystal grown from

THF solution. Comparison of the metrical parameters for the phosphonium cations of **13** and **14** reveals that they are identical within experimental error. The closest contact between P^+ and I_3^- is 3.883(6) Å. Although no mechanistic information is available, it is plausible that the interaction of dipp-BIAN with PI_3 results in the initial formation of I_2 and “[dipp-BIAN)PI]”, from which I^- is abstracted by I_2 . As in the case of **13**, subsequent or concomitant intramolecular charge transfer affords the final product, **14**.

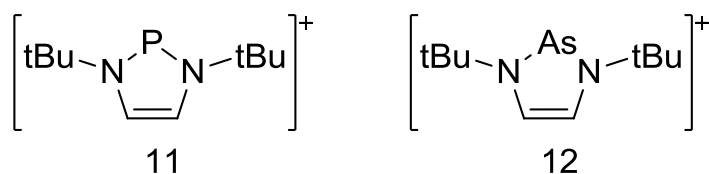


Figure 1.12. Depiction of previously reported phosphonium^{5,14} and arsenium cation¹⁶.

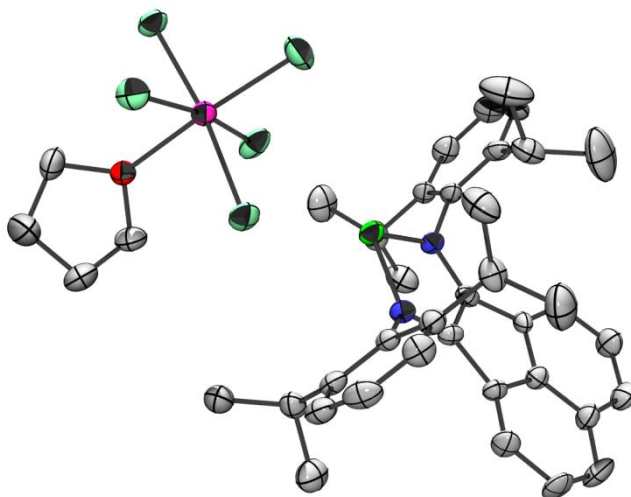


Figure 1.13. Molecular structure of **15**. The thermal ellipsoids are shown at the 40% probability level. All hydrogen atoms have been omitted for clarity.

The arsenium salt [(dipp-BIAN)As][SnCl₅THF] **15** was prepared by a similar procedure to that employed for the synthesis of **13**. The green crystalline product was

examined by single-crystal X-ray diffraction (Figure 1.13). The AsN₂C₂ ring is planar, and the average C-N and As-N bond distances are very similar to those in **12**^{5,14,16} (Figure 1.12) and subsequently reported³⁶ cyclic arsenium cations, thus supporting the view that arsenic is in the +3 oxidation state. The fact that the C(1)-C(12) bond distances in **13**, **14**, and **15** are 0.06 Å longer than the corresponding distances in **11** and **12** (Figure 1.06) is presumably due to the constraints of the somewhat rigid dipp-BIAN framework. Finally, it is noteworthy that the [(dipp-BIAN)As]⁺ cation is isoelectronic with [(dipp-BIAN)Ge].³⁷ As expected, the N-E-N bond angle and E-N bond distances are smaller for the arsenic cation than the corresponding germylene due to the fact that the ionic radius of As³⁺ is less than that of Ge²⁺. As in the case of **13**, the shortest cation-anion contacts involve As-Cl(1) (3.298(5) Å) and As-Cl(2) (3.215(5) Å).

*Synthesis and Characterization of [(DippBIAN)P]⁺[SnCl₅•THF]⁻ (**13**)*

The salt [(DippBIAN)P]⁺[SnCl₅•THF]⁻ (**13**) was prepared by stirring a solution of PCl₃ and SnCl₂ in THF (20 mL) for 3 h at ambient temperature. A solution of DippBIAN in THF (30 mL) was added dropwise to this mixture over a period of 30 min. The reaction mixture was then stirred for 12 h and subsequently filtered through Celite®. Workup of the reaction mixture and removal of solvent under reduced pressure resulted in the isolation of an analytically pure red-brown powder in 66% yield. Recrystallization of the crude product by slow diffusion of *n*-hexane into a THF solution of **13** afforded a crop of dark green crystals suitable for single-crystal X-ray diffraction study which confirmed the identity of the title compound to be that displayed in Figure 1.14. Details of the data collection, structure solution and refinement have been compiled in Table 1.19 and a selection of pertinent metrical parameters is presented in Tables 1.20 and 1.21.

Compound **13** crystallizes in the monoclinic space group $P2_1/n$. The metrical parameters which are pertinent to the description of the structure of **13** include the C(1)-C(12) bond distance of 1.395(5) Å, which is indicative of a C-C double bond, and the average C-N bond distance of 1.359(5) Å which implies a bond order of one. As expected, these metrical parameters are similar to those of previously reported N-heterocyclic phosphonium cations.

A $^{31}\text{P}\{^1\text{H}\}$ NMR spectroscopic analysis revealed the presence of a signal located at δ : 232.5. The chemical shift of this signal is indicative of the presence of a phosphonium cation and is consistent with those of previously reported examples.

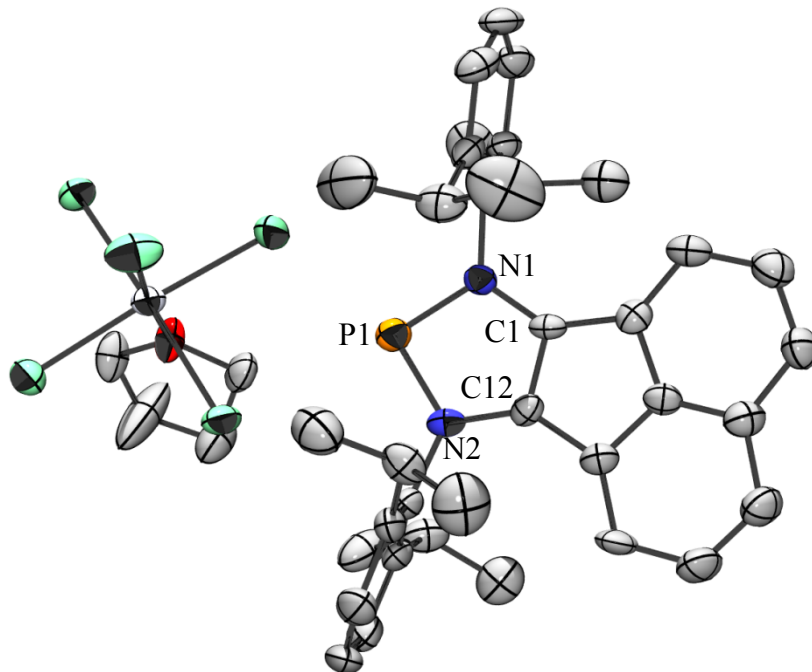


Figure 1.14. Molecular structure of 13 showing a partial numbering scheme. The thermal ellipsoids are shown at the 40% probability level. All hydrogen atoms have been omitted for clarity.

Synthesis and Characterization of [(DippBIAN)P]⁺[I₃]⁻ (14)

The salt [(DippBIAN)P]⁺[I₃]⁻ (**14**) was prepared by dropwise addition of a solution of PI₃ in 30 mL of CH₂Cl₂ to a solution of DippBIAN in 30 mL of CH₂Cl₂ over a period of 30 min. The resulting red-brown reaction mixture was stirred for 12 h, following which it was filtered through Celite®. Workup of the reaction mixture and removal of the solvent under reduced pressure, followed by washing twice with Et₂O resulted in the isolation of **14** as an analytically pure light brown powder in 70% yield. Recrystallization of **14** from a dichloromethane/hexane (2:1) mixture at -40 °C under an argon atmosphere afforded a crop of light brown crystals suitable for single-crystal X-ray diffraction experiments. The X-ray diffraction study confirmed the identity of the product to be that of the title compound shown in Figure 1.15. Details of the data collection, structure solution and refinement are presented in Table 1.22 and selections of metrical parameters are listed in Tables 1.23 and 1.24.

Compound **14** crystallizes in the monoclinic space group *P2₁/c*. The metrical parameters which are pertinent to the description of the structure of **14** include the C(1)-C(12) bond distance of 1.380(8) Å, which is indicative of a C-C double bond, and the average C-N bond distance of 1.358(7) Å which implies a bond order of one. As expected, these metrical parameters are similar to those of previously reported N-heterocyclic phosphonium cations.

Analysis by ³¹P{¹H} NMR revealed the presence of a signal located at δ: 234.5. The chemical shift of this signal is indicative of the presence of a phosphonium cation and is consistent with those of previously reported examples.

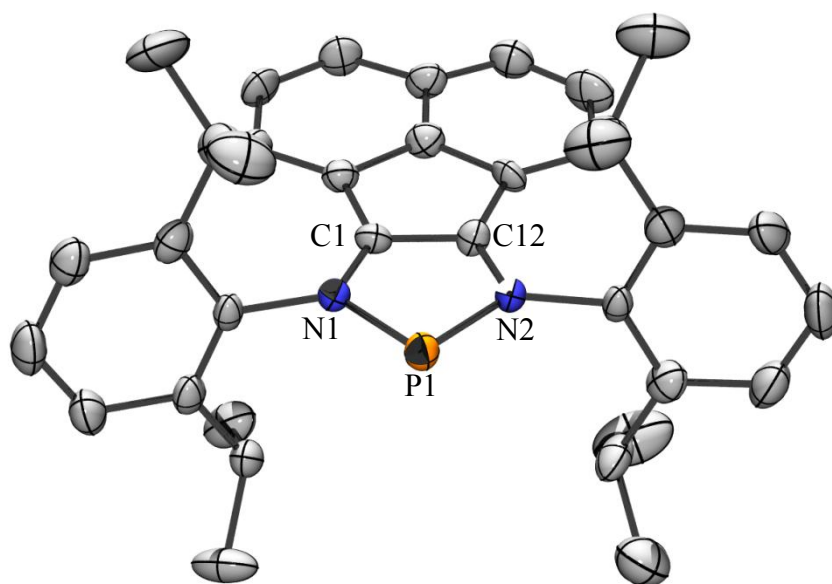


Figure 1.15. Molecular structure of 14 showing a partial numbering scheme. The thermal ellipsoids are shown at the 40% probability level. All hydrogen atoms and the I_3^- counter-anion have been omitted for clarity.

Synthesis and Characterization of [(DippBIAN)As]⁺[SnCl₅•THF]⁻ (15)

The salt [(DippBIAN)As]⁺[SnCl₅•THF]⁻ (**15**) was synthesized by stirring a mixture of AsCl₃ and SnCl₂ in THF solution (20 mL) for 3 h at ambient temperature. A solution of DippBIAN in THF (30 mL) was added dropwise to the aforementioned mixture over a period of 30 min. The resulting reaction mixture was stirred for 12 h, following which it was filtered through Celite®. Workup of the reaction mixture followed by removal of solvent under reduced pressure resulted in the isolation of an emerald green powder (yield = 90%). Recrystallization of the crude product by slow evaporation of a THF solution under an atmosphere of argon afforded a crop of dark green crystals suitable for X-ray diffraction experiments. A single-crystal X-ray diffraction study confirmed the identity of the title compound to be that shown in Figure

1.16. Details of the data collection, structure solution and refinement are compiled in Table 1.25 and selections of metrical parameters are listed in Tables 1.26 and 1.27.

Compound **15** crystallizes in the monoclinic space group $P2_1/n$. The metrical parameters which are pertinent to the description of the structure of **15** include the C(1)-C(12) bond distance of 1.399(6) Å, which is indicative of a C-C double bond, and the average C-N bond distance of 1.348(5) Å which implies a bond order of one. As expected, these metrical parameters are similar to those of previously reported N-heterocyclic arsenium cations.

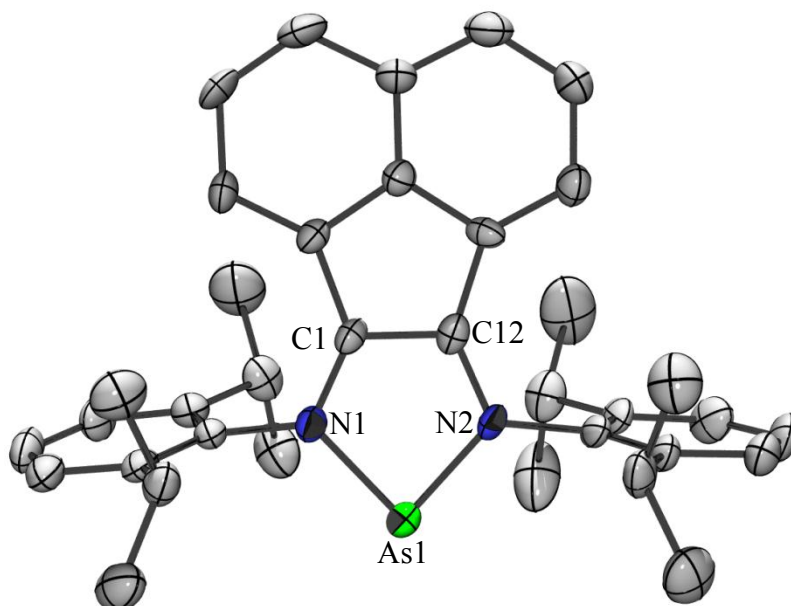


Figure 1.16. Molecular structure of 15 showing a partial numbering scheme. The thermal ellipsoids are shown at the 40% probability level. All hydrogen atoms and the SnCl_5^- counter-anion have been omitted for clarity.

EXPERIMENTAL SECTION

General Procedures

The solvents toluene, THF and hexanes were distilled over sodium along with a sodium benzophenone ketyl indicator and degassed prior to use. Dichloromethane was distilled over calcium hydride and degassed prior to use. Concentrated acetic acid and acetonitrile were used without purification. An M-Braun argon-filled drybox was employed for the manipulation of all air-sensitive solid reagents. All reactions requiring anaerobic conditions were performed using standard Schlenk or drybox techniques. All glassware was dried at least 24 h in a 120 °C oven prior to use. All the ligands used in this work were synthesized according to the pertinent literature procedures.

Physical Measurements

Low-resolution chemical ionization (CI) mass spectral (MS) data were collected on a Finnigan MAT TSQ-700 mass spectrometer, and high-resolution CIMS spectra were recorded on a VG Analytical ZAB-VE sector instrument. All MS analyses were performed on samples that had been sealed in glass capillaries under an Ar atmosphere. Solution-phase NMR spectra were recorded at 298 K on a Varian Inova instrument (^1H NMR, 300.14 MHz; $^{13}\text{C}\{^1\text{H}\}$ NMR, 75.48 MHz; $^{31}\text{P}\{^1\text{H}\}$ NMR, 121.52 MHz) immediately following removal of the samples from a drybox. The ^1H and $^{13}\text{C}\{^1\text{H}\}$ chemical shift values are reported in parts per million (ppm) relative to SiMe_4 (δ : 0.00), using residual solvent resonances as internal standards. The $^{31}\text{P}\{^1\text{H}\}$ chemical shift values are reported relative to external 85% H_3PO_4 .

X-ray Crystallography

Crystals of **4**, **6-10**, and **13-15** were removed from Schlenk flasks under a positive pressure of argon, placed on glass slides, covered with degassed hydrocarbon oil, and mounted on thin nylon loops. The X-ray diffraction data were collected at 153 K on a Nonius Kappa CCD area detector diffractometer equipped with an Oxford Cryostream low-temperature device and a graphite-monochromated Mo-KR radiation source ($\lambda = 0.71073 \text{ \AA}$). Corrections were applied for Lorentz and polarization effects. All six structures were solved by direct methods and refined by full-matrix least-squares cycles on $F=2.22$. All non-hydrogen atoms were refined with anisotropic thermal parameters, and H atoms were placed in fixed, calculated positions using a riding model (C-H 0.96 \AA). The total number of reflections, collection ranges and final R-values for each structure are listed in the appropriate crystallographic data tables.

General Synthetic Procedures for 4-8

A solution of PI_3 in 30 mL of CH_2Cl_2 was added dropwise to a solution of the appropriate R-diimine ligand in 30 mL of CH_2Cl_2 over a period of 30 min. The reaction mixture was stirred for 12 h, following which it was filtered through Celite®. Removal of the volatiles under reduced pressure resulted in the isolation of the powdered products, which were subsequently recrystallized from a 2:1 dichloromethane/hexane mixture at $-40 \text{ }^\circ\text{C}$ under an argon atmosphere.

4. The reaction of PI_3 (0.758 g, 1.48 mmol) with $(t\text{-Bu})\text{NC}(\text{H})\text{C}(\text{H})\text{N}(t\text{-Bu})$ (0.310 g, 1.48 mmol) resulted in the isolation of 0.9 g (84%) of dark brown powder **4**. ^1H NMR (300.14 MHz, CDCl_3): δ 1.84 [s, 18H, CH_3], 7.94 [s, 2 H, $\text{CH}=\text{CH}$]. $^{13}\text{C}\{^1\text{H}\}$ NMR (75.48 MHz, CDCl_3): δ 31.33 [d, $3J(^{13}\text{C}-^{31}\text{P}) = 9.4 \text{ Hz}$, $\text{CH}-3$], 62.47 [$\text{C}(\text{CH}_3)$], 131.11 [$\text{C}=\text{C}$]. $^{31}\text{P}\{^1\text{H}\}$ NMR (121.52 MHz, CDCl_3): δ 204.3. LRMS (CI^+ , m/z) (%): 323 (100%,

t-Bu-DABP⁺), 143 (38%, *t*-Bu-DABP⁺-*t*-Bu). HRMS (CI+, CH₄): calcd for C₁₀H₂₀N₂P⁺, 199.1365; found, 199.1365.

5. The reaction of PI₃ (0.467 g, 1.13 mmol) with (*p*-tol)NC-(Me)C(Me)N(*p*-tol) (0.300 g, 1.13 mmol) afforded 0.68 g (88%) of dark-brown powder 5. ¹H NMR (300.14 MHz, CDCl₃): δ 2.37 [s, 6 H, CH₃], 2.49 [s, 6 H, CH₃], 7.43-7.58 [m, 4 H, H_{arom}]. ¹³C-¹H NMR (75.48 MHz, CDCl₃): δ 14.20, 21.66, 127.20 [*J*(¹³C-³¹P) = 5.0 Hz], 131.09, 131.47 [*J*(¹³C-³¹P) = 12.2 Hz], 140.99, 141.73. ³¹P{¹H} NMR (121.52 MHz, CDCl₃): δ 227.1. LRMS (CI+, *m/z*) (%): 323 (100%, *p*-tol-DABP⁺). HRMS (CI+, CH₄): calcd for C₁₈H₂₀N₂P⁺, 295.1364; found, 295.1364.

6. The reaction of PI₃ (1.41 g, 3.42 mmol) with (Mes)NC(H)C-(H)N(Mes) (1 g, 3.42 mmol) resulted in 2.1 g (87%) of brown powder 6. ¹H NMR (300.14 MHz, CDCl₃): δ 2.25 [s, 12 H, CH₃], 2.41 [s, 6 H, CH₃], 7.17 [s, 4 H, H_{arom}-Mes], 7.94 [s, 2 H, CH=CH]. ¹³C{¹H} NMR (75.48 MHz, CDCl₃): δ 18.64, 21.28 [CH₃], 130.60, 131.70 [*J*(¹³C-³¹P) = 6.6 Hz], 134.11 [*J*(¹³C-³¹P) = 3.2 Hz], 136.23 [*J*(¹³C-³¹P) = 2.7 Hz], 141.89 [C_{arom}]. ³¹P{¹H} NMR (121.52 MHz, CDCl₃): δ 209.7. LRMS (CI+, *m/z*) (%): 323 (100%, Mes-DABP⁺). LRMS (CI-, *m/z*) (%): 127 (100%, I). HRMS (CI+, CH₄): calcd for C₂₀H₂₄N₂P⁺, 323.1677; found, 323.1677.

7. The reaction of PI₃ (1.09 g, 2.66 mmol) with (2,6-*i*-Pr₂C₆H₃)-NC(H)C(H)(2,6-*i*-Pr₂C₆H₃) (1 g, 2.66 mmol) afforded 1.9 g (92%) of brown powder 7. ¹H NMR (300.14 MHz, CDCl₃): δ 1.36 [d, 3*J*(¹H-¹H) = 6.9 Hz, 24 H, CH₃], 2.69 [m, 4 H, CH], 7.42-7.45 [m, 4 H, C_{arom}-dipp], 7.63 [m, 2 H, C_{arom}-dipp], 8.05 [s, 2 H, HC=CH]. ¹³C{¹H} NMR (75.48 MHz, CDCl₃): δ 24.73, 25.72, 29.32 [*i*-Pr], 125.19, 130.48, 131.98, 136.26, 145.19 [C_{arom}]. ³¹P{¹H} NMR (121.52 MHz, CDCl₃): δ 207.4. LRMS (CI+, *m/z*) (%): 407 (100%, dippDABP⁺). LRMS (CI-, *m/z*) (%): 127 (100%, I). HRMS (CI+, CH₄): calcd for C₂₆H₃₆N₂P⁺, 407.2616; found, 407.2617 (0.1 ppm).

8. The reaction of PI_3 (0.374 g, 0.91 mmol) with $(\text{Cy})\text{NC}(\text{H})\text{C}(\text{H})\text{N}(\text{Cy})$ (0.2 g, 0.91 mmol) resulted in 0.46 g (81%) of brown powder **8**. ^1H NMR (300.14 MHz, CDCl_3): δ 1.39 [tt, 2 H, H_{Cy}], 1.60 [qt, 4 H, H_{Cy}], 1.81-2.05 [complex pattern, 10 H, H_{Cy}], 2.51 [mult, 4 H, H_{Cy}], 4.95 [m, 2 H, H_{Cy}], 7.97 [s, 2 H, $\text{CH}=\text{CH}$]. $^{13}\text{C}\{^1\text{H}\}$ NMR (75.48 MHz, CDCl_3): δ 24.74, 25.28 [$J(^{13}\text{C}-^{31}\text{P})$ 1.7 Hz], 35.47 [$J(^{13}\text{C}-^{31}\text{P})$ 8.83 Hz], 62.31 [$J(^{13}\text{C}-^{31}\text{P})$ 9.9 Hz], 132.15 [$J(^{13}\text{C}-^{31}\text{P})$ 3.9 Hz]. $^{31}\text{P}\{^1\text{H}\}$ NMR (121.52 MHz, CDCl_3): δ 209.9. LRMS (CI^+ , m/z) (%): 251 (35%, Cy-DABP^+). HRMS (CI^+ , CH_4): calcd for $\text{C}_{14}\text{H}_{24}\text{N}_2\text{P}^+$, 251.1677; found, 251.1676.

General Synthetic Procedures for **11** and **12**

A mixture of the appropriate phosphonium triiodide salt and NaBPh_4 in 50 mL of THF solution was stirred at room temperature for 12 h. All volatiles were removed under reduced pressure, and the resulting yellow residue was extracted with 30 mL of CH_2Cl_2 to give a clear light-yellow solution. Slow evaporation of the solvent under an argon atmosphere resulted in the crystalline tetraphenylborate salts **11** and **12** in virtually quantitative yields.

11. The reaction of NaBPh_4 (0.342 g, 1.03 mmol) with **4** (0.2 g, 0.345 mmol) resulted in a virtually quantitative yield of colorless crystalline **11**. ^1H NMR (300.14 MHz, CD_2Cl_2): δ 1.61 [s, 18 H, CH_3], 6.87 [m, 4 H, BPh_4^-], 7.02 [m, 8 H, BPh_4^-], 7.94 [s, 2 H, $\text{CH}=\text{CH}$], 7.33 [m, 8 H, BPh_4^-]. $^{13}\text{C}\{^1\text{H}\}$ NMR (75.48 MHz, CD_2Cl_2): δ 31.42 [d, $3J(^{13}\text{C}-^{31}\text{P})$ 9.3 Hz], CH_3], 63.15 [$2J(^{13}\text{C}-^{31}\text{P})$ 7.7 Hz, $\text{C}(\text{CH}_3)$], 122.12 [BPh_4^-], 125.95 [BPh_4^-], 132.79 [$\text{C}=\text{C}$], 136.22 [BPh_4^-], 164,19 [BPh_4^-]. $^{31}\text{P}\{^1\text{H}\}$ NMR (121.52 MHz, CD_2Cl_2): δ 202.5. LRMS (CI^+ , m/z) (%): 199 (50%, $t\text{-Bu-DABP}^+$), 165 (100%, Ph_2B^+). HRMS (CI^+ , CH_4): calcd for $\text{C}_{10}\text{H}_{20}\text{N}_2\text{P}^+$, 199.1365; found, 199.1365.

12. The reaction of NaBPh₄ (0.26 g, 0.762 mmol) with **7** (0.2 g, 0.254 mmol) resulted in a virtually quantitative yield of light-yellow crystals of **12**. ¹H NMR (300.14 MHz, CDCl₃): δ 1.19 [d, 3*J*(¹H-¹H)) 6.9 Hz, 12 H, CH₃], 1.32 [d, 3*J*(¹H-¹H)) 6.9 Hz, 12 H, CH₃], 2.22 [m, 4 H, CH], 6.10 [d, 3*J*(¹H-³¹P)) 1.2 Hz, 2 H, HC=CH], 6.74 [t, 4 H, H_{arom}(BPh₄)], 6.90 [t, 8 H, H_{arom}(BPh₄)], 7.38-7.43 [m, 14 H, H_{arom}(BPh₄) and H_{arom}(dipp)]. ¹³C{¹H} NMR (75.48 MHz, CDCl₃): δ 21.72, 24.23, 27.28 [*i*-Pr], 120.37, 123.09 [BPh₄⁻], 124.02 [BPh₄⁻], 130.42, 134.58 [BPh₄⁻], 136.96, 137.67, 142.88, 162.3 [BPh₄⁻]. ³¹P{¹H} NMR (121.52 MHz, CDCl₃): δ 204.4 (br). LRMS (CI+, *m/z*) (%): 484 (100%, dipp-DABP+Ph), 407 (61%, dipp-DABP⁺). LRMS (CI-, *m/z*) (%): 243 (30%, BPh₃). HRMS (CI+, CH₄): calcd for C₂₆H₃₆N₂P⁺, 407.2616; found, 407.2626.

Synthesis of [(DippBIAN)P]⁺[SnCl₅•THF]⁻

13. A mixture of PCl₃ (0.218 g, 2 mmol) and SnCl₂ (0.379 g, 2 mmol) in THF solution (20 mL) was stirred for 3 h at ambient temperature. A solution of dippBIAN (1 g, 2 mmol) in THF (30 mL) was added dropwise to this solution over a period of 30 min. The resulting yellow-brown reaction mixture was stirred for 12 h. Removal of all the volatiles afforded a red/brown solid (1.1 g, 66 %). Dark green single crystals were obtained by slow diffusion of *n*-hexane into a THF solution of **13**. ¹H NMR (300.14 MHz, CD₂Cl₂): δ 1.18 (d, 3*J*_{HH} 6.6 Hz, 12H, Me), 1.35 (d, 3*J*_{HH} = 6.9 Hz, 12H, Me), 2.69 (m, 4 H, CH), 7.16 (d, 3*J*_{HH} = 7.2 Hz, 2H, H(3)), 7.55 – 7.75 (m, 6 H, H_{arom}-dipp), 7.83 (m, 2H, H(4)), 8.20 (d, 3*J*_{HH} = 8.4 Hz, 2H, H(5)). ¹³C{¹H} NMR (75.48 MHz, CD₂Cl₂): δ 23.88, 25.83, 29.99 (*i*-Pr), 123.70 (d, *J*_{CP} = 4.5 Hz) 125.03 (d, *J*_{CP} = 3.1 Hz), 148.37 (C_{arom}). ³¹P{¹H} NMR (121.52 MHz, CD₂Cl₂): δ 232.5(s). LRMS (CI+, CH₄): *m/z* 566 (25 %, [(dipp-BIAN)PCl]), 531 (100%, [(dipp-BIAN)P]⁺), 501 (80 %, dipp-BIAN), 457

(20 %, dipp-BIAN-*i*-Pr). LRMS (CI-, CH₄): *m/z* 295 (100 %, SnCl₅⁻), 260 (10 %, SnCl₄). HRMS (CI+, CH₄) calcd for C₃₆H₄₀N₂P⁺, 531.2929; found 531.2949.

Synthesis of [(DippBIAN)P]⁺[I₃]⁻

14. A solution of PI₃ (0.823 g, 2 mmol) in CH₂Cl₂ (20 mL) was added dropwise to a solution of dipp-BIAN (1 g, 2 mmol) in CH₂Cl₂ (30 mL) at 25°C over a period of 30 min. The dark brown reaction mixture was stirred for 12 h. Removal of all the volatiles afforded a dark brown solid which was washed twice with Et₂O (20 mL) and once with pentane (20 mL). The residual solid was dried under reduced pressure yielding a light brown powder (1.26 g, 70 %). ¹H NMR (300.14 MHz, CD₂Cl₂): δ 1.17 (*d*, 3 J_{HH} = 6.9 Hz, 12H, Me), 1.36 (*d*, 3 J_{HH} = 6.9 Hz, 12H, Me), 2.71 (*m*, 4H, CH), 7.16 (*d*, 3 J_{HH} = 7.2 Hz, 2H, H(3)), 7.55 – 7.75 (*m*, 6H, H_{arom}-dipp), 7.82 (*m*, 2H, H(4)), 8.19 (*d*, 3 J_{HH} = 8.4 Hz, 2H, H(5)). ¹³C {¹H} NMR (75.48, CD₂Cl₂): δ 23.96, 25.89, 29.97 (*i*-Pr), 123.80 (*d*, 3 J_{CP} = 4.5 Hz), 124.99 (*d*, J_{CP} = 8.8 Hz), 126.23, 129.90 (*d*, J_{CP} = 7.2 Hz), 129.44, 130.97, 132.79, 133.30, 135.11, 145.13 (*d*, J_{CP} = 1.4 Hz), 148.29 (C_{arom}). ³¹P {¹H} NMR (121.52 MHz, CD₂Cl₂): δ 234.5(*s*). LRMS (CI+, CH₄): *m/z* 531 (100%, (dipp- BIAN)P⁺); LRMS (CI-, CH₄): *m/z* 127 (100%, I⁻). HRMS (CI+, CH₄) calcd for C₃₆H₄₀N₂P⁺ 531.2929; found 531.2935.

Synthesis of [(DippBIAN)As]⁺[SnCl₅•THF]⁻

15. A solution of AsCl₃ (0.181 g, 1 mmol) and SnCl₂ (0.189 g, 1 mmol) in THF solution (20 mL) was stirred for 3 h at ambient temperature. A solution of dipp-BIAN (0.5 g, 1 mmol) in THF (30 mL) was added dropwise to this mixture over a period of 30 min. The resulting yellow-green reaction mixture was stirred for 12 h. Removal of all the

volatiles afforded an emerald-green solid (0.55 g, 90 %). Single crystals were obtained by slow evaporation of a THF solution of **15** under a stream of argon. ^1H NMR (300.14, CD_2Cl_2): δ 1.14 (d, $J_{\text{HH}} = 6.9$ Hz, 12H, Me), 1.39 (d, $3J_{\text{HH}} = 6.9$ Hz, 12H, Me), 2.79 (m, 4H, CH), 6.99 (d, $3J_{\text{HH}} = 7.5$ Hz, 2H, H(3)), 7.60 – 7.68 (m, 6H, $\text{H}_{\text{arom-dipp}}$), 7.81 (m, 2H, H(4)), 8.15 (d, $3J_{\text{HH}} = 8.4$ Hz, 2H, H(5)). $^{13}\text{C}\{^1\text{H}\}$ NMR (75.48 MHz, CD_2Cl_2): δ 24.21, 25.73, 29.84 (*i*-Pr), 124.58, 125.62, 125.98, 129.22, 131.08, 132.11, 132.48, 132.92, 136.58, 144.34, 150.97 (C_{arom}). LRMS (CI^+ , CH_4): m/z 610 (20 %, [dipp-BIAN)As-Cl], 576 (100%, (dipp-BIAN)As $^+$), 501 (30 %, dipp-BIAN), 458 (50 %, dipp-BIAN-*i*-Pr). LRMS (CI^- , CH_4): m/z 295 (100 %, SnCl_5^-), 260 (45 %, SnCl_4), 225 (60 %, SnCl_3^-). HRMS (CI^+ , CH_4) calcd for $\text{C}_{36}\text{H}_{40}\text{N}_2\text{As}^+$ 575.2407; found 575.2401.

TABLES OF CRYSTALLOGRAPHIC DATA

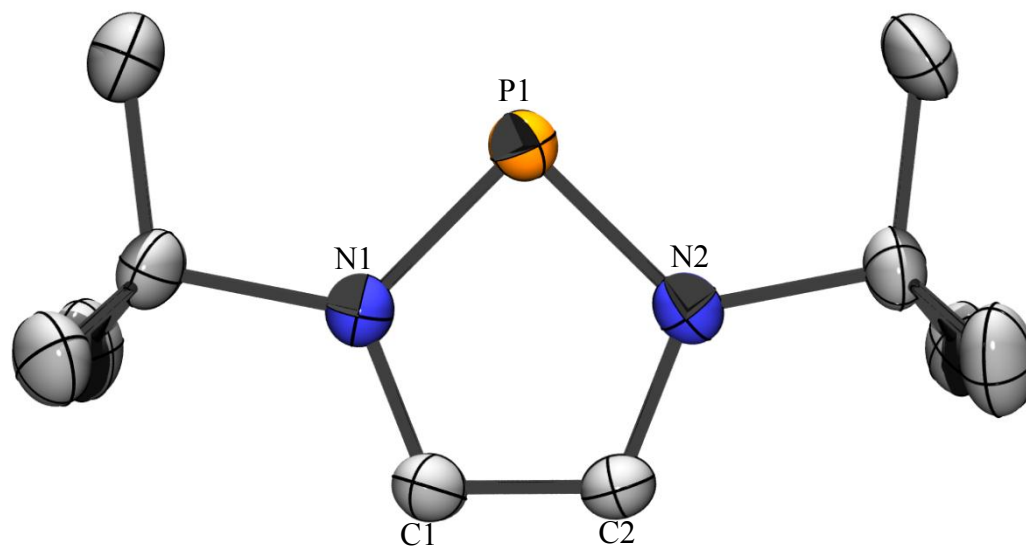


Figure 1.17. Molecular structure of 4 showing a partial numbering scheme. The thermal ellipsoids are shown at the 40% probability level. All hydrogen atoms and the I_3^- counter-anion have been omitted for clarity.

Table 1.01. Crystal data and structure refinement for 4.

Empirical formula	C ₁₄ H ₂₈ I ₃ N ₂ OP	
Formula weight	652.05	
Temperature	153(2)K	
Wavelength	0.710 69 Å	
Crystal system	monoclinic	
Space group	<i>P21/c</i>	
Unit cell dimensions	a = 12.993(5)	α = 90°
	b = 15.126(5)	β = 110.922(5)°
	c = 12.254(5)	λ = 90°
Volume	2249.5(15)Å ³	
Z	4	
Density (calculated)	1.925 g cm ⁻³	
Absorption coefficient	4.241 mm ⁻¹	
F(000)	1232	
Theta ranges for data collection	2.15 – 27.50	
Reflections collected	9040	
Independent reflections	5151	
Refinement method	Full-matrix least-squares on F ²	
Data / restraints / parameters	5151/0/200	
Goodness of-fit on F ²	1.078	
Final R indices [I>2σ(I)]	0.0341, 0.0738	
R indices (all data)	0.0635, 0.0845	
Largest diff. peak and hole	0.893/-0.871	

Table 1.02. Selected bond lengths (Å) for 4.

C(1)–C(2)	1.353(6)
N(1)–C(1)	1.366(5)
N(2)–C(2)	1.373(5)
N(1)–P(1)	1.664(3)
N(2)–P(1)	1.663(4)

Table 1.03. Selected bond angles (°) for 4.

N(1)–P(1)–N(2)	90.14(17)
N(1)–C(1)–C(2)	111.3(4)
N(2)–C(2)–C(1)	111.7(4)

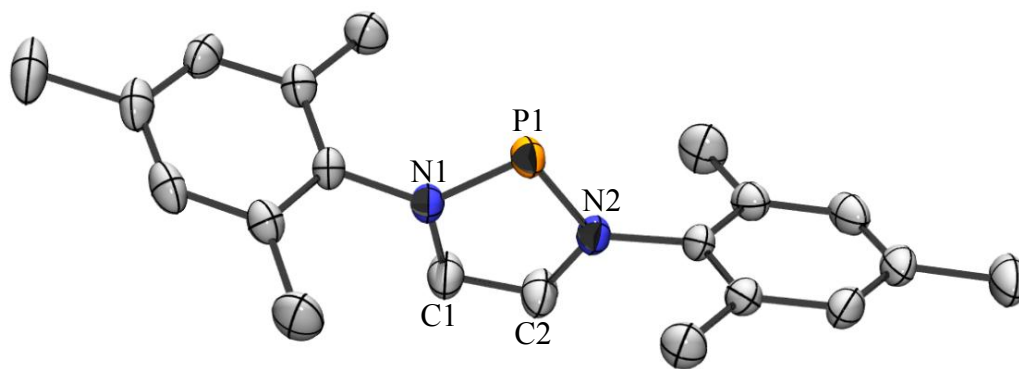


Figure 1.18. Molecular structure of 6 showing a partial numbering scheme. The thermal ellipsoids are shown at the 40% probability level. All hydrogen atoms and the I₃⁻ counter-anion have been omitted for clarity.

Table 1.04. Crystal data and structure refinement for 6.

Empirical formula	C ₂₀ H ₂₄ I ₃ N ₂ P	
Formula weight	704.08	
Temperature	153(2)K	
Wavelength	0.710 69 Å	
Crystal system	monoclinic	
Space group	<i>C2/c</i>	
Unit cell dimensions	a = 21.647(4)	$\alpha = 90^\circ$
	b = 7.5469(15)	$\beta = 112.69(3)^\circ$
	c = 16.488(3)	$\lambda = 90^\circ$
Volume	2249.5(15)Å ³	
Z	4	
Density (calculated)	1.882 g cm ⁻³	
Absorption coefficient	3.884 mm ⁻¹	
F(000)	1328	
Theta ranges for data collection	2.68 – 27.45	
Reflections collected	4601	
Independent reflections	2828	
Refinement method	Full-matrix least-squares on F ²	
Data / restraints / parameters	2828/0/123	
Goodness of-fit on F ²	1.065	
Final R indices [I>2sigma(I)]	0.0446, 0.1129	
R indices (all data)	0.0609, 0.1244	
Largest diff. peak and hole	1.831/-1.796	

Table 1.05. Selected bond lengths (Å) for 6.

C(1)–C(2)	1.342(9)
N(1)–C(1)	1.371(6)
N(2)–C(2)	1.371(6)
N(1)–P(1)	1.665(3)
N(2)–P(1)	1.665(3)

Table 1.06. Selected bond angles (°) for 6.

N(1)–P(1)–N(2)	89.4(2)
N(1)–C(1)–C(2)	111.4(2)
N(2)–C(2)–C(1)	111.4(2)

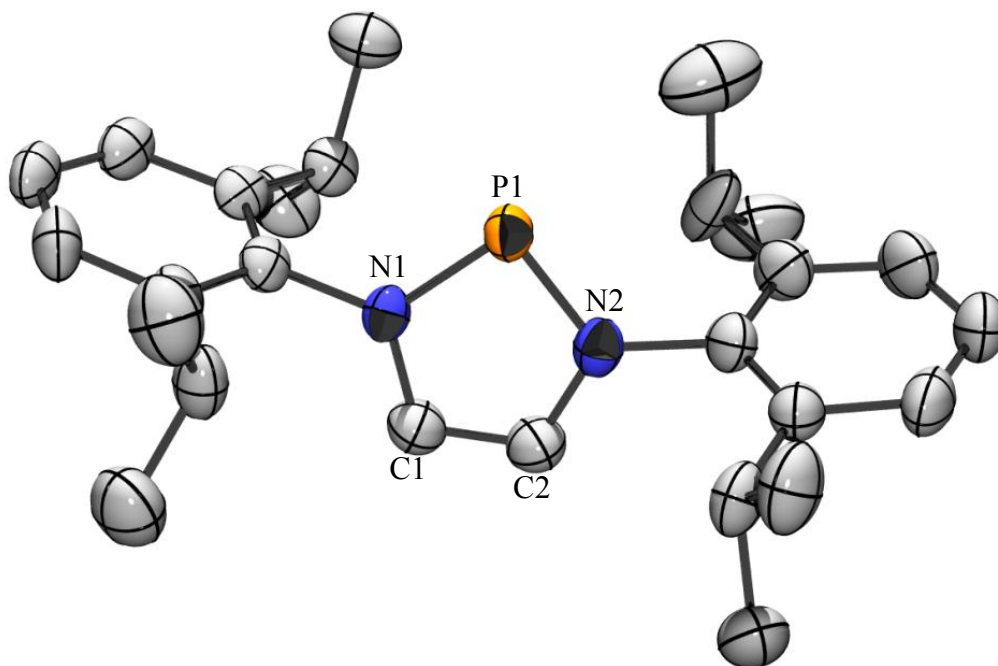


Figure 1.19. Molecular structure of 7 showing a partial numbering scheme. The thermal ellipsoids are shown at the 40% probability level. All hydrogen atoms and the I_3^- counter-anion have been omitted for clarity.

Table 1.07. Crystal data and structure refinement for 7.

Empirical formula	C ₂₆ H ₃₆ I ₃ N ₂ P	
Formula weight	788.24	
Temperature	153(2)K	
Wavelength	0.710 69 Å	
Crystal system	monoclinic	
Space group	<i>P</i> 1	
Unit cell dimensions	a = 9.861(5)	α = 89.522(5)°
	b = 10.501(5)	β = 78.766(5)°
	c = 16.856(5)	λ = 80.179(5)°
Volume	1686.4(13)Å ³	
Z	2	
Density (calculated)	1.552 g cm ⁻³	
Absorption coefficient	2.842 mm ⁻¹	
F(000)	760	
Theta ranges for data collection	1.97 – 27.50	
Reflections collected	12191	
Independent reflections	7642	
Refinement method	Full-matrix least-squares on F ²	
Data / restraints / parameters	7642/0/297	
Goodness of-fit on F ²	1.107	
Final R indices [I>2σ(I)]	0.0450, 0.1163	
R indices (all data)	0.0820, 0.1267	
Largest diff. peak and hole	0.931/-1.082	

Table 1.08. Selected bond lengths (Å) for 7.

C(1)–C(2)	1.342(6)
N(1)–C(1)	1.376(6)
N(2)–C(2)	1.400(5)
N(1)–P(1)	1.674(4)
N(2)–P(1)	1.673(4)

Table 1.09. Selected bond angles (°) for 7.

N(1)–P(1)–N(2)	89.75(17)
N(1)–C(1)–C(2)	111.5(4)
N(2)–C(2)–C(1)	111.5(4)

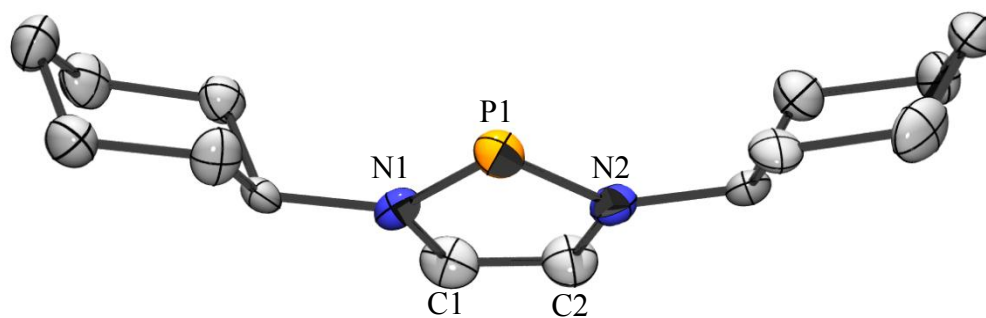


Figure 1.20. Molecular structure of 8 showing a partial numbering scheme. The thermal ellipsoids are shown at the 40% probability level. All hydrogen atoms and the I₃⁻ counter-anion have been omitted for clarity.

Table 1.10. Crystal data and structure refinement for 8.

Empirical formula	C ₁₄ H ₂₄ I ₃ N ₂ P	
Formula weight	632.02	
Temperature	153(2)K	
Wavelength	0.710 69 Å	
Crystal system	triclinic	
Space group	<i>P</i> 1	
Unit cell dimensions	a = 13.817(5)	α = 82.750(5)°
	b = 17.943(5)	β = 68.210(5)°
	c = 18.382(5)	λ = 70.130(5)°
Volume	3980(2)Å ³	
Z	8	
Density (calculated)	2.110 g cm ⁻³	
Absorption coefficient	4.787mm ⁻¹	
F(000)	2368	
Theta ranges for data collection	2.95 – 27.50	
Reflections collected	28143	
Independent reflections	18017	
Refinement method	Full-matrix least-squares on F ²	
Data / restraints / parameters	18017/0/721	
Goodness of-fit on F ²	1.103	
Final R indices [I>2σ(I)]	0.0641, 0.1462	
R indices (all data)	0.1169, 0.1651	
Largest diff. peak and hole	1.817/-1.541	

Table 1.11. Selected bond lengths (Å) for 8.

C(1)–C(2)	1.344(17)
N(1)–C(1)	1.388(15)
N(2)–C(2)	1.370(15)
N(1)–P(1)	1.673(10)
N(2)–P(1)	1.679(10)

Table 1.12. Selected bond angles (°) for 8.

N(1)–P(1)–N(2)	89.4(5)
N(1)–C(1)–C(2)	112.7(11)
N(2)–C(2)–C(1)	110.4(10)

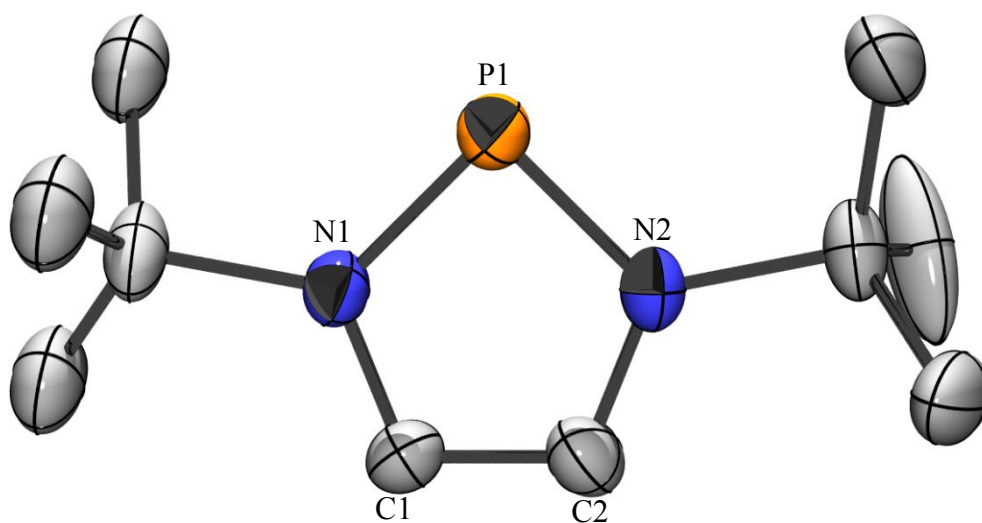


Figure 1.21. Molecular structure of 11 showing a partial numbering scheme. The thermal ellipsoids are shown at the 40% probability level. All hydrogen atoms and the BPh₄⁻ counter-anion have been omitted for clarity.

Table 1.13. Crystal data and structure refinement for 11.

Empirical formula	C ₃₄ H ₃₈ BN ₂ P	
Formula weight	516.44	
Temperature	153(2)K	
Wavelength	0.710 69 Å	
Crystal system	orthorhombic	
Space group	<i>Pbca</i>	
Unit cell dimensions	a = 9.7482(19)	α = 90°
	b = 17.553(4)	β = 90°
	c = 34.013(7)	λ = 90°
Volume	5820(2)Å ³	
Z	8	
Density (calculated)	1.179 g cm ⁻³	
Absorption coefficient	0.120 mm ⁻¹	
F(000)	2208	
Theta ranges for data collection	2.40 – 27.47	
Reflections collected	11712	
Independent reflections	6425	
Refinement method	Full-matrix least-squares on F ²	
Data / restraints / parameters	6425/7/350	
Goodness of-fit on F ²	1.023	
Final R indices [I>2σ(I)]	0.0672, 0.1755	
R indices (all data)	0.1130, 0.2051	
Largest diff. peak and hole	0.562 /-0.528	

Table 1.14. Selected bond lengths (Å) for 11.

C(1)–C(2)	1.352(4)
N(1)–C(1)	1.371(3)
N(2)–C(2)	1.365(4)
N(1)–P(1)	1.668(2)
N(2)–P(1)	1.656(2)

Table 1.15. Selected bond angles (°) for 11.

N(1)–P(1)–N(2)	90.09(11)
N(1)–C(1)–C(2)	110.6(3)
N(2)–C(2)–C(1)	112.3(3)

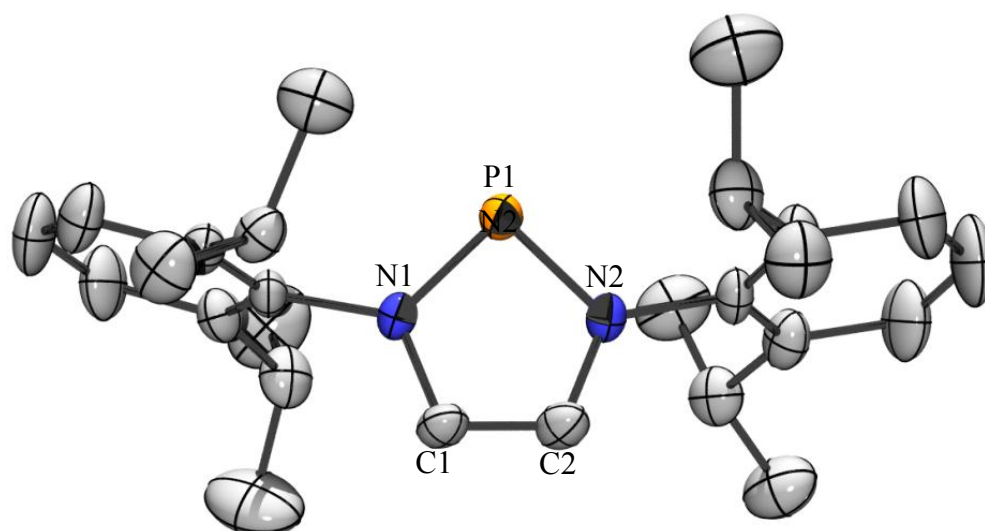


Figure 1.22. Molecular structure of 12 showing a partial numbering scheme. The thermal ellipsoids are shown at the 40% probability level. All hydrogen atoms and the BPh_4^- counter-anion have been omitted for clarity.

Table 1.16. Crystal data and structure refinement for 12.

Empirical formula	C ₅₀ H ₅₆ BN ₂ P	
Formula weight	726.75	
Temperature	153(2)K	
Wavelength	0.710 69 Å	
Crystal system	monoclinic	
Space group	<i>P</i> 2 ₁ / <i>c</i>	
Unit cell dimensions	a = 20.593(5)	α = 90°
	b = 17.673(5)	β = 91.069(5)°
	c = 23.597(5)	λ = 90°
Volume	8569(4)Å ³	
Z	8	
Density (calculated)	1.127 g cm ⁻³	
Absorption coefficient	0.099 mm ⁻¹	
F(000)	3120	
Theta ranges for data collection	1.52 – 27.49	
Reflections collected	33860	
Independent reflections	19610	
Refinement method	Full-matrix least-squares on F ²	
Data / restraints / parameters	19610/4/1005	
Goodness of-fit on F ²	1.014	
Final R indices [I>2σ(I)]	0.0553, 0.1102	
R indices (all data)	0.1124, 0.1314	
Largest diff. peak and hole	0.327 /-0.322	

Table 1.17. Selected bond lengths (Å) for 12.

C(1)–C(2)	1.355(3)
N(1)–C(1)	1.387(3)
N(2)–C(2)	1.370(4)
N(1)–P(1)	1.686(2)
N(2)–P(1)	1.664(3)

Table 1.18. Selected bond angles (°) for 12.

N(1)–P(1)–N(2)	89.22(12)
N(1)–C(1)–C(2)	111.5(3)
N(2)–C(2)–C(1)	111.0(2)

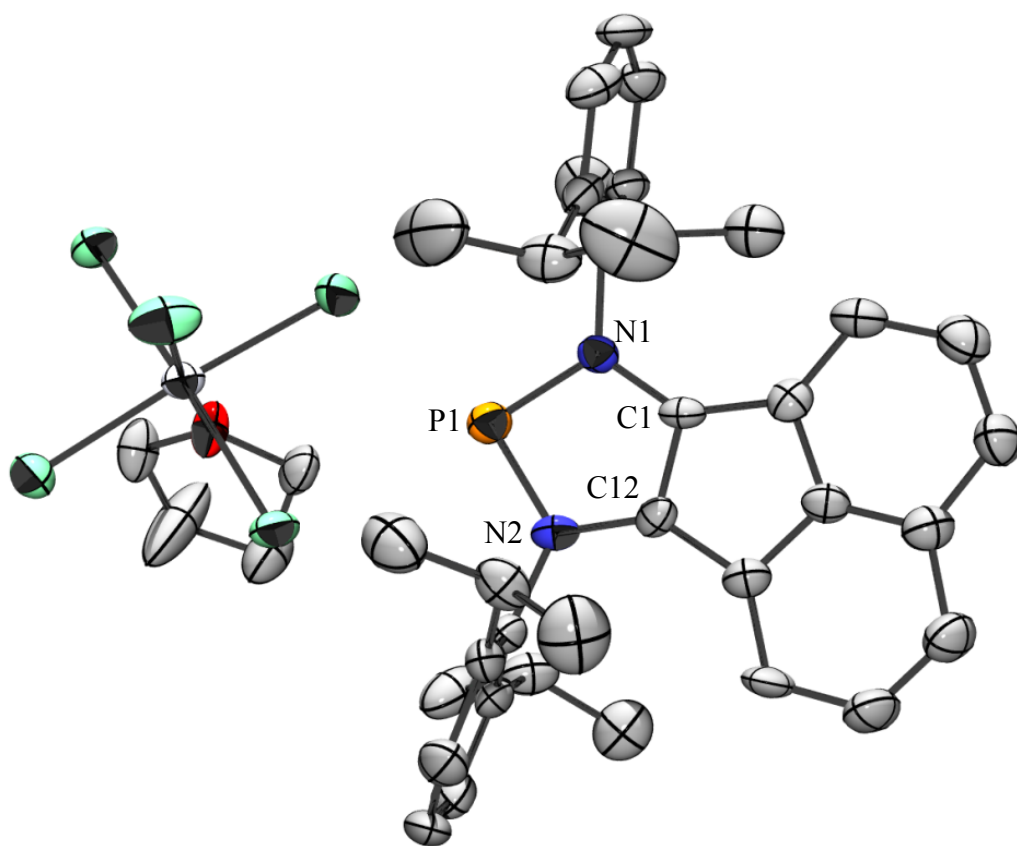


Figure 1.14. Molecular structure of 13 showing a partial numbering scheme. The thermal ellipsoids are shown at the 40% probability level. All hydrogen atoms have been omitted for clarity.

Table 1.19. Crystal data and structure refinement for 13.

Empirical formula	C ₄₀ H ₄₈ Cl ₅ N ₂ OPSn	
Formula weight	899.7	
Temperature	153(2)K	
Wavelength	0.710 73 Å	
Crystal system	monoclinic	
Space group	<i>P2₁/n</i>	
Unit cell dimensions	a = 13.189(5)	α = 90°
	b = 22.335(5)	β = 104.102(5)°
	c = 14.637(5)	λ = 90°
Volume	4182(2)Å ³	
Z	4	
Density (calculated)	1.429 g cm ⁻³	
Absorption coefficient	1.002 mm ⁻¹	
Reflections collected	15498	
Independent reflections	8180	
Refinement method	Full-matrix least-squares on F ²	
Goodness of-fit on F ²	0.979	
Final R indices [I>2σ(I)]	0.0471	
R indices (all data)	0.0995	

Table 1.20. Selected bond lengths (Å) for 13.

C(1)–C(12)	1.395(5)
N(1)–C(1)	1.351(5)
N(2)–C(12)	1.366(5)
N(1)–P(1)	1.694(4)
N(2)–P(1)	1.689(4)

Table 1.21. Selected bond angles (°) for 13.

N(1)–P(1)–N(2)	90.23(17)
N(1)–C(1)–C(12)	112.3(4)
N(2)–C(12)–C(1)	110.9(4)

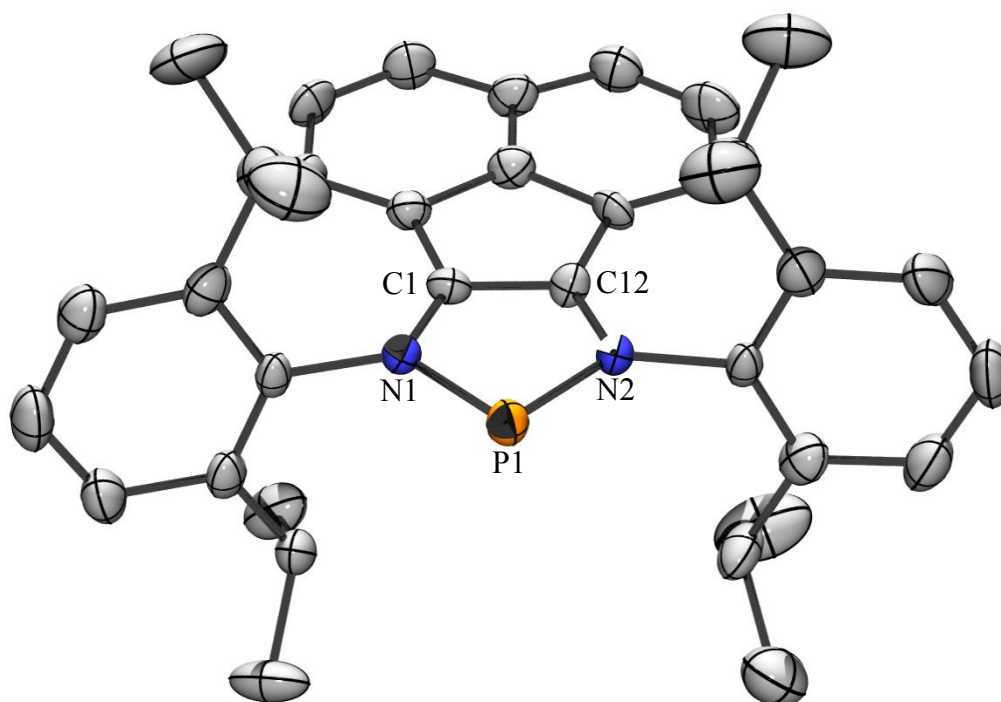


Figure 1.15. Molecular structure of 14 showing a partial numbering scheme. The thermal ellipsoids are shown at the 40% probability level. All hydrogen atoms and the I_3^- counter-anion have been omitted for clarity.

Table 1.22. Crystal data and structure refinement for 14.

Empirical formula	C ₃₆ H ₄₀ I ₃ N ₂ P	
Formula weight	912.40	
Temperature	153(2)K	
Wavelength	0.710 73 Å	
Crystal system	monoclinic	
Space group	<i>P2₁/c</i>	
Unit cell dimensions	a = 17.625(4)	α = 90°
	b = 15.265(3)	β = 114.03(3)°
	c = 17.014(3)	λ = 90°
Volume	4180.5(15)Å ³	
Z	2	
Density (calculated)	1.450 g cm ⁻³	
Absorption coefficient	2.304 mm ⁻¹	
Reflections collected	17430	
Independent reflections	9546	
Refinement method	Full-matrix least-squares on F ²	
Goodness of-fit on F ²	0.927	
Final R indices [I>2σ(I)]	0.0478	
R indices (all data)	0.1202	

Table 1.23. Selected bond lengths (Å) for 14.

C(1)–C(12)	1.380(8)
N(1)–C(1)	1.354(7)
N(2)–C(12)	1.361(7)
N(1)–P(1)	1.700(4)
N(2)–P(1)	1.685(4)

Table 1.24. Selected bond angles (°) for 14.

N(1)–P(1)–N(2)	89.75(2)
N(1)–C(1)–C(12)	111.8(5)
N(2)–C(12)–C(1)	111.7(5)

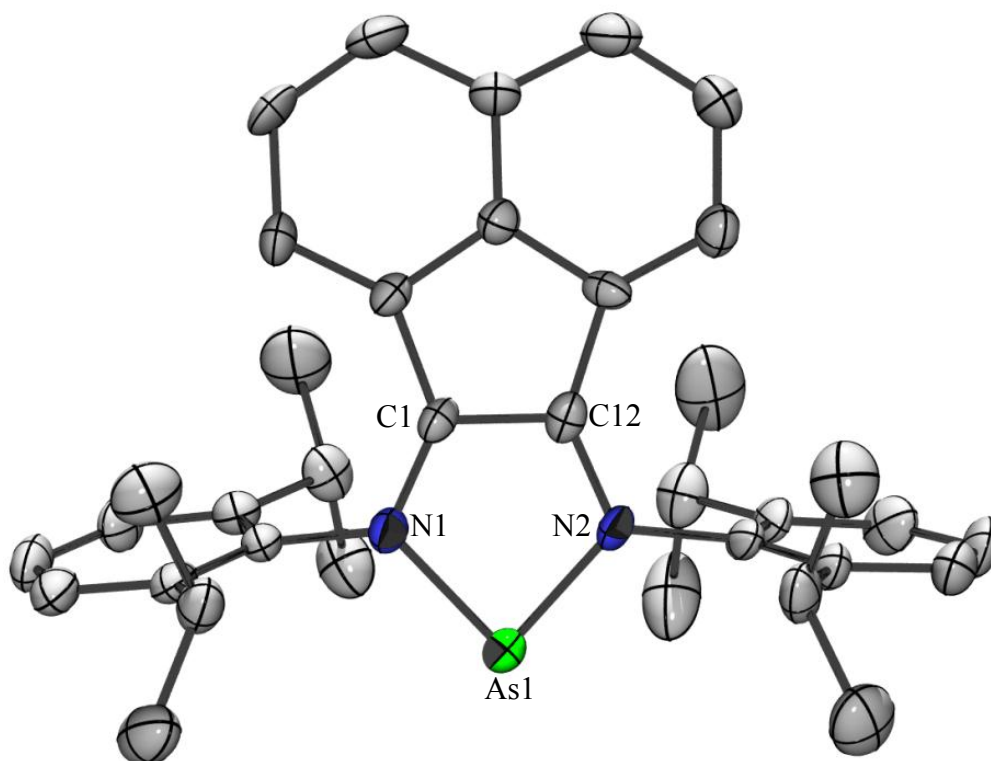


Figure 1.16. Molecular structure of 15 showing a partial numbering scheme. The thermal ellipsoids are shown at the 40% probability level. All hydrogen atoms and the SnCl_5^- counter-anion have been omitted for clarity.

Table 1.25. Crystal data and structure refinement for 15.

Empirical formula	C ₄₀ H ₄₈ Cl ₅ N ₂ OAsSn	
Formula weight	943.72	
Temperature	153(2)K	
Wavelength	0.710 73 Å	
Crystal system	monoclinic	
Space group	<i>P2₁/n</i>	
Unit cell dimensions	a = 13.317(5)	α = 90°
	b = 22.302(5)	β = 103.936(5)°
	c = 14.546(5)	λ = 90°
Volume	4193.5(2)Å ³	
Z	4	
Density (calculated)	1.495 g cm ⁻³	
Absorption coefficient	1.744 mm ⁻¹	
Reflections collected	16547	
Independent reflections	9460	
Refinement method	Full-matrix least-squares on F ²	
Goodness of-fit on F ²	0.985	
Final R indices [I>2σ(I)]	0.0512	
R indices (all data)	0.0831	

Table 1.26. Selected bond lengths (Å) for 15.

C(1)–C(12)	1.399(6)
N(1)–C(1)	1.348(5)
N(2)–C(12)	1.348(5)
N(1)–As(1)	1.839(3)
N(2)–As(1)	1.857(4)

Table 1.27. Selected bond angles (°) for 15.

N(1)–As(1)–N(2)	84.89(15)
N(1)–C(1)–C(12)	112.6(4)
N(2)–C(12)–C(1)	115.3(4)

References

- (1) Cowley, A. H.; Kemp, R. A. *Chemical Reviews* **1985**, *85*, 367.
- (2) Rauzy, K.; Mazieres, M. R.; Page, P.; Sanchez, M.; Bellan, J. *Tetrahedron Letters* **1990**, *31*, 4463.
- (3) Gudat, D. *Coordination Chemistry Reviews* **1997**, *163*, 71.
- (4) Herrmann, W. A. *Angewandte Chemie International Edition* **2002**, *41*, 1290.
- (5) Gudat, D.; Haghverdi, A.; Hupfer, H.; Nieger, M. *Chemistry – A European Journal* **2000**, *6*, 3414.
- (6) Hardman, N. J.; Abrams, M. B.; Pribisko, M. A.; Gilbert, T. M.; Martin, R. L.; Kubas, G. J.; Baker, R. T. *Angewandte Chemie International Edition* **2004**, *43*, 1955.
- (7) Abrams, M. B.; Scott, B. L.; Baker, R. T. *Organometallics* **2000**, *19*, 4944.
- (8) Sakakibara, K.; Yamashita, M.; Nozaki, K. *Tetrahedron Letters* **2005**, *46*, 959.
- (9) Breit, B. *Journal of Molecular Catalysis A: Chemical* **1999**, *143*, 143.
- (10) Litvinov, I. A.; Naumov, V. A.; Griaznova, T. V.; Pudovik, A. N.; Kibardin, A. M. *Doklady Akademii Nauk SSSR* **1990**, *312*, 623.
- (11) Arduengo, A. J.; Harlow, R. L.; Kline, M. *Journal of the American Chemical Society* **1991**, *113*, 361.
- (12) Kibardin, A. M.; Litvinov, I. A.; Naumov, V. A.; Struchkov, I. T.; Griaznova, T. V.; Mikhailov, I. B.; Pudovik, A. N. *Doklady Akademii Nauk SSSR* **1988**, *298*, 369.
- (13) Denk, M. K.; Gupta, S.; Ramachandran, R. *Tetrahedron Letters* **1996**, *37*, 9025.
- (14) Denk, M. K.; Gupta, S.; Lough, A. J. *European Journal of Inorganic Chemistry* **1999**, *1999*, 41.
- (15) Gudat, D.; Holderberg, A. W.; Kotila, S.; Nieger, M. *Chemische Berichte* **1996**, *129*, 465.
- (16) Carmalt, C.; Lomeli, V. *Chemical Communications* **1997**, 2095.
- (17) Burck, S.; Gudat, D.; Nieger, M.; Du Mont, W.-W. *Journal of the American Chemical Society* **2006**, *128*, 3946.
- (18) Schmidpeter, A.; Lochschmidt, S.; Sheldrick, W. S. *Angewandte Chemie International Edition in English* **1982**, *21*, 63.
- (19) Schmidpeter, A.; Lochschmidt, S.; Sheldrick, W. S. *Angewandte Chemie International Edition in English* **1985**, *24*, 226.
- (20) Boon, J. A.; Byers, H. L.; Dillon, K. B.; Goeta, A. E.; Longbottom, D. A. *Heteroatom Chemistry* **2000**, *11*, 226.
- (21) Barnham, R. J.; Deng, R. M. K.; Dillon, K. B.; Goeta, A. E.; Howard, J. A. K.; Puschmann, H. *Heteroatom Chemistry* **2001**, *12*, 501.

- (22) Ellis, B. D.; Dyker, C. A.; Decken, A.; Macdonald, C. L. B. *Chemical Communications* **2005**, 1965.
- (23) Ellis, B. D.; Carlesimo, M.; Macdonald, C. L. B. *Chemical Communications* **2003**, 1946.
- (24) Ellis, B. D.; Macdonald, C. L. B. *Inorganic Chemistry* **2006**, *45*, 6864.
- (25) Lochschmidt, S.; Schmidpeter, A. *Z Naturforsch B* **1985**, *40*, 765.
- (26) Fedushkin, I. L.; Skatova, A. A.; Chudakova, V. A.; Fukin, G. K. *Angewandte Chemie International Edition* **2003**, *42*, 3294.
- (27) van Laren, M. W.; Elsevier, C. J. *Angewandte Chemie International Edition* **1999**, *38*, 3715.
- (28) van Belzen, R.; Hoffmann, H.; Elsevier, C. J. *Angewandte Chemie International Edition in English* **1997**, *36*, 1743.
- (29) Shirakawa, E.; Hiyama, T. *Journal of Organometallic Chemistry* **2002**, *653*, 114.
- (30) Schumann, H.; Hummert, M.; Lukoyanov, A. N.; Fedushkin, I. L. *Organometallics* **2005**, *24*, 3891.
- (31) Ellis, B. D.; Macdonald, C. L. B. *Inorgica Chimica Acta* **2007**, *360*, 329.
- (32) Burford, N.; Losier, P.; Macdonald, C.; Kyrimis, V.; Bakshi, P. K.; Cameron, T. S. *Inorganic Chemistry* **1994**, *33*, 1434.
- (33) El-Ayaan, U.; Paulovicova, A.; Fukuda, Y. *Journal of Molecular Structure* **2003**, *645*, 205.
- (34) Marsh, R. *Acta Crystallographica Section B* **2004**, *60*, 252.
- (35) Fedushkin, I. L.; Chudakova, V. A.; Skatova, A. A.; Khvoynova, N. M.; Kurskii, Y. A.; Glukhova, T. A.; Fukin, G. K.; Dechert, S.; Hummert, M.; Schumann, H. *Zeitschrift für anorganische und allgemeine Chemie* **2004**, *630*, 501.
- (36) Gans-Eichler, T.; Gudat, D.; Nieger, M. *Heteroatom Chemistry* **2005**, *16*, 327.
- (37) Fedushkin, I. L.; Skatova, A. A.; Chudakova, V. A.; Khvoynova, N. M.; Baurin, A. Y.; Dechert, S.; Hummert, M.; Schumann, H. *Organometallics* **2004**, *23*, 3714.

Vita

Clint Russell Hoberg was born in El Centro, California on October 18, 1981, the son of Cynthia Enz and Donn Hoberg. After graduating from Holtville High School, Holtville, California in 1999, he attended The University of Arizona, Tucson, Arizona and received the degree of Bachelor of Science in Chemistry in May 2004. In August 2004, he entered the Graduate School of The University of Texas at Austin.

Permanent address (or email): 9801 Stonelake Blvd. #1913

Austin, TX 78759

This thesis was typed by the author.